

## **General Disclaimer**

### **One or more of the Following Statements may affect this Document**

- This document has been reproduced from the best copy furnished by the organizational source. It is being released in the interest of making available as much information as possible.
- This document may contain data, which exceeds the sheet parameters. It was furnished in this condition by the organizational source and is the best copy available.
- This document may contain tone-on-tone or color graphs, charts and/or pictures, which have been reproduced in black and white.
- This document is paginated as submitted by the original source.
- Portions of this document are not fully legible due to the historical nature of some of the material. However, it is the best reproduction available from the original submission.

5030-567

Electric & Hybrid Vehicle System  
Research & Development Project

DOE/CS-54209-13

Distribution Category UC-96

(NASA-CR-173726) PERFORMANCE OF THE LESTER  
BATTERY CHARGER IN ELECTRIC VEHICLES (Jet  
Propulsion Lab.) 54 p HC A04/MF A01

N84-27982

CSCL 09A

Unclass  
19835

G3/33

# Performance of the Lester Battery Charger in Electric Vehicles

H.C. Vivian  
J.A. Bryant

April 15, 1984

Prepared for  
U.S. Department of Energy  
Through an Agreement with  
National Aeronautics and Space Administration  
by  
Jet Propulsion Laboratory  
California Institute of Technology  
Pasadena, California

JPL Publication 84-4



5030-567  
Electric & Hybrid Vehicle System  
Research & Development Project

DOE/CS-54209-13  
Distribution Category UC-96

# Performance of the Lester Battery Charger in Electric Vehicles

H.C. Vivian  
J.A. Bryant

April 15, 1984

Prepared for  
U.S. Department of Energy  
Through an Agreement with  
National Aeronautics and Space Administration  
by  
Jet Propulsion Laboratory  
California Institute of Technology  
Pasadena, California

JPL Publication 84-4

Prepared by the Jet Propulsion Laboratory, California Institute of Technology,  
for the U.S. Department of Energy through an agreement with the National  
Aeronautics and Space Administration.

This report was prepared as an account of work sponsored by an agency of the  
United States Government. Neither the United States Government nor any  
agency thereof, nor any of their employees, makes any warranty, express or  
implied, or assumes any legal liability or responsibility for the accuracy, com-  
pleteness, or usefulness of any information, apparatus, product, or process  
disclosed, or represents that its use would not infringe privately owned rights.

Reference herein to any specific commercial product, process, or service by trade  
name, trademark, manufacturer, or otherwise, does not necessarily constitute or  
imply its endorsement, recommendation, or favoring by the United States  
Government or any agency thereof. The views and opinions of authors  
expressed herein do not necessarily state or reflect those of the United States  
Government or any agency thereof.

Work conducted through NASA Task RE-152, Amendment 170 and sponsored  
by the U.S. Department of Energy under Interagency Agreement  
DE-A101-78CS54209.

## ABSTRACT

Tests were performed on an improved battery charger manufactured by Lester Electrical of Nebraska, Inc. This charger was installed in a South Coast Technology Rabbit No. 4, which was equipped with lead-acid batteries produced by ESB Company. The primary purpose of the testing was to develop test methodologies for battery charger evaluation. To this end tests were developed to characterize the charger in terms of its charge algorithm and to assess the effects of battery initial state of charge and temperature on charger and battery efficiency. Tests showed this charger to be a considerable improvement in the state of the art for electric vehicle chargers.

## ACKNOWLEDGMENT

The detailed contents of this report would not have been possible without the diligent efforts of several people. D. Palmeiri directed the test program in the Automotive Research Facility of the California Institute of Technology (Caltech), Jet Propulsion Laboratory (JPL), in Pasadena, California; he was assisted by R. Burleson and L. Johnson. Data and document preparation were done by B. Bonzo and T. McMillian. The authors are grateful for the contribution supplied by each of these people.

## CONTENTS

I.	INTRODUCTION . . . . .	1-1
II.	SUMMARY . . . . .	2-1
	A. CONCLUSIONS . . . . .	2-1
	B. RECOMMENDATIONS . . . . .	2-2
III.	CHARGER DESCRIPTION . . . . .	3-1
	A. PHYSICAL CHARACTERISTICS . . . . .	3-1
	B. ELECTRICAL CHARACTERISTICS . . . . .	3-1
	C. CHARGE ALGORITHM . . . . .	3-3
IV.	TEST PROGRAM AND METHODOLOGY . . . . .	4-1
V.	DISCUSSION . . . . .	5-1
	A. CHARGE ALGORITHM . . . . .	5-1
	B. EFFICIENCIES . . . . .	5-4
	C. CHARGER WAVEFORMS . . . . .	5-9
VI.	CONCLUSIONS AND RECOMMENDATIONS . . . . .	6-1
	A. CONCLUSIONS . . . . .	6-1
	B. RECOMMENDATIONS . . . . .	6-1
	REFERENCES . . . . .	7-1
APPENDIXES		
	A. DATA SUMMARY OF TESTS ON LESTER CHARGER WITH EXIDE BATTERIES . . . . .	A-1
	B. CALCULATED DATA: CHARGER AND BATTERY THROUGHPUT EFFICIENCIES . . . . .	B-1

C.	CHARGER/BATTERY RECHARGE CHARACTERISTICS FOR SEVERAL TESTS . . . . .	C-1
D.	TYPICAL OSCILLOGRAPHS OR CHARGER INPUT AND OUTPUT POWER VS. AMPERE-HOUR CHARGES . . . . .	D-1
E.	CHARGER INPUT POWER WAVEFORM AND FOURIER ANALYSES VS. CHARGER LOAD CURRENTS . . . . .	E-1
F.	OPERATION MANUAL, PARTS LIST, AND SCHEMATIC FOR MODEL 9865 LESTER CHARGER . . . . .	F-1



## SECTION I

### INTRODUCTION

The Jet Propulsion Laboratory (JPL) conducts research and development activities as well as vehicle and system-level testing for the Department of Energy (DOE) Electric and Hybrid Vehicle (EHV) Program. Part of JPL's responsibility is the development and testing of battery chargers used on electric vehicles (EV). In response to this requirement, JPL contracted with Gould, Inc., to develop an advanced Battery Charger/State-of-Charge Indicator (BC/SCI) (Reference 1). Subsequently, an attempt was made during 1981 to compile test data from other chargers to use as a basis for comparison with the Gould BC/SCI. However, due to unreliable characteristics of the battery chargers in the vehicles previously tested by JPL (Reference 2), this could not be done.

Later in 1981, JPL received several R-1 electric vehicles from South Coast Technology (SCT), Detroit, Michigan. These cars were equipped with an improved charger. Routine use of these new SCT vehicles revealed these chargers to be reliable after some early problems were overcome. Because of a general lack of objective battery charger performance data, one of the chargers manufactured by Lester Electrical of Nebraska, Inc., (Lester) was installed in the SCT vehicles and subjected to a brief series of tests. The main objectives of this testing were to develop baseline data against which the Gould charger could be compared and to develop a methodology for determining battery charger performance.

This report presents these findings. It includes the results of a brief test series that was developed to evaluate a charger's efficiency when charging is initiated at various battery depths of discharge (DoD) and various battery temperatures. A description of the charger and its control algorithm is also included. No attempt is made to quantify the charger's electromagnetic interference or radio frequency interference characteristics.

Although the primary objective of this testing was to develop an evaluation methodology, much useful information was also gained about the performance of the Lester charger.

## SECTION II

### SUMMARY

Tests on the Lester battery charger were conducted at JPL as a pathfinder activity in the development of a test methodology to assess the developmental Gould charger. The test program also provided a data base against which the Gould, or any other, charger could be compared. Performance of the charger versus battery DoD and electrolyte temperature was evaluated. However, problems with the test setup severely limited the intended temperature variations, which precluded any meaningful assessment of the charger's temperature-dependent performance.

#### A. CONCLUSIONS

During testing, the Lester charger performed well and consistently. After an initial failure problem, which was quickly repaired by Lester, the charger operated reliably for more than 2 years. The following conclusions were derived from this test program:

- (1) Lester's charge algorithm represents a considerable improvement over any commercially available charge controls known to the authors to date.
- (2) The charger itself (Figure 2-1) is reasonably efficient. Although other more efficient chargers are commercially available, their lack of a precise charge algorithm can result in a poorer overall battery/charger efficiency.
- (3) During conditions of shallow discharge, the combined charger and battery efficiencies decrease because of the fixed, 50-min period at the end of charge. It has been JPL's experience that the finish-charge duration can be shortened following shallow discharges.
- (4) The lack of electrolyte temperature compensation will impair the quality and efficiency of recharge when battery temperature deviates from the nominal 27°C (80°F) for which the charge algorithm was developed. It is postulated that, when the temperature is above approximately 46°C (115°F), battery voltage will not rise to the 124-V lid at which current tapering is initiated. Therefore, charging would continue at the high 32-A rate until the voltage-rate change (dv/dt) charge termination criterion is satisfied. The opposite problem will occur at colder battery temperatures. Both of these temperature-related charging problems are detrimental to the battery's life and/or performance.
- (5) The technique of reducing the isolation transformer's flux by increasing the winding gap is an inefficient method of achieving current limiting.

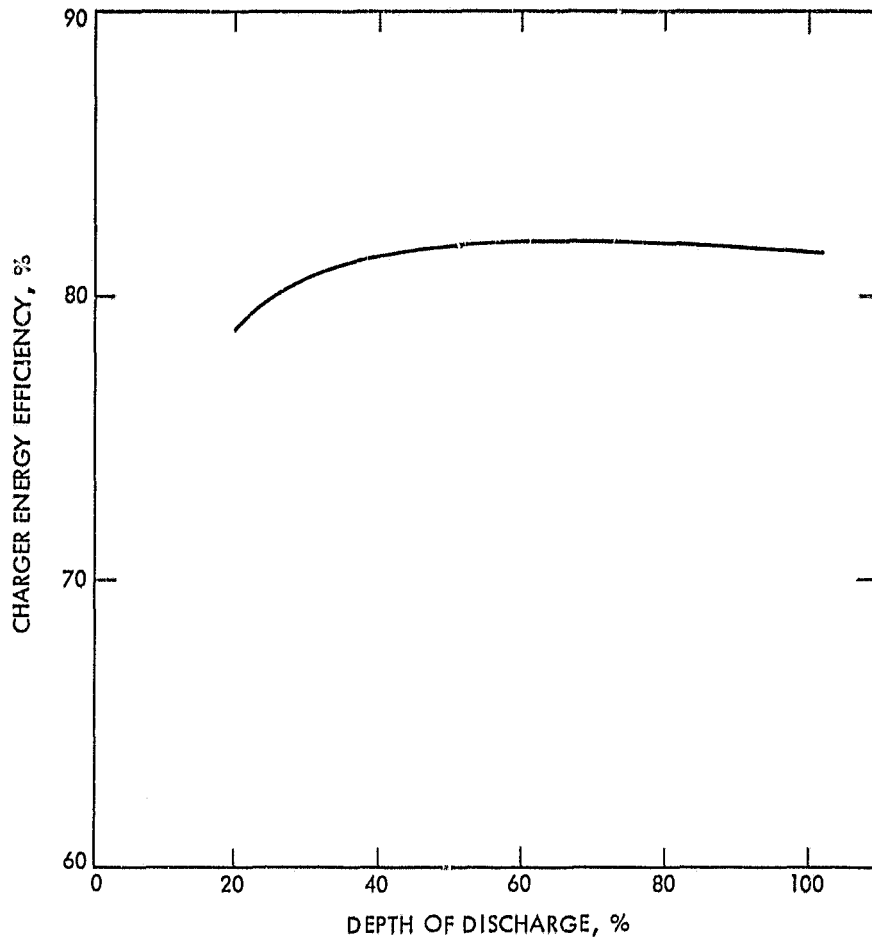


Figure 2-1. Charger Energy Efficiency at Various Depths of Discharge

#### B. RECOMMENDATIONS

The objectives of the test program were not fully satisfied because the effect of battery temperature on battery charge/discharge and charger efficiency was not investigated. However, the following recommendations are valid until additional testing, at different temperatures, proves otherwise:

- (1) Charge algorithms, for lead-acid batteries in particular, must compensate for battery temperature unless their temperature is controlled to a specific value. Unless recharge is compensated, the battery will probably be overcharged or undercharged. In either case, battery performance, life, and/or maintainance will suffer.
- (2) Some charging testing should be performed at elevated and reduced battery temperatures to quantify the severity of the problem for this particular charge algorithm.

- (3) Lester could investigate an improved design for the charger's isolation transformer. Coupling efficiency and power factor could thereby be enhanced, improving charger throughput efficiency.
- (4) In general, the whole area of battery charging requires more attention. Considering the relative benefits of developing improved charge algorithms versus the cost of development, charge algorithm development would be a cost-effective and worthwhile effort.

## SECTION III

### CHARGER DESCRIPTION

Lester was selected by SCT to provide an improved battery charger for the R-1 electric vehicles. This charger was tailored to physical constraints of the SCT vehicle and to the charging requirements dictated by ESB Corporation for its XPV-23 battery. Each of these general characteristics is discussed in separate subsections. Operation of the charger is discussed in Appendix A.

#### A. PHYSICAL CHARACTERISTICS

Figure 3-1 shows the charger as it is installed in the SCT vehicle. It can be seen that the controls, indicators, and fuses are all relatively accessible. Figures 3-2 and 3-3 show different views of the charger itself. Table 3-1 provides the physical specifications for the charger.

#### B. ELECTRICAL CHARACTERISTICS

Figure 3-4 shows the major electrical components of the Lester charger. The input transformer is designed so that 115-Vac or 208/230-Vac power can be used. However, the charger is designed primarily for use with a 208/230-Vac circuit. The 115-Vac input circuitry is intended for emergency use only if the higher voltage circuits are not available. Much of the automatic operation

Table 3-1. Lester Electrical Charger Physical Specifications

---

Size	
Height	27.9 cm (11.0 in.)
Width	20.3 cm (8.0 in.)
Length (excludes fan) <sup>a</sup>	41.9 cm (16.4 in.)
Weight	
Total (includes fan)	33.6 kg (74 lb)

---

<sup>a</sup>As shown in Figure 3-3, the fan is mounted external to the charger chassis. It could be located almost anywhere on the charger and is, therefore, not included in the dimensions.

---



Figure 3-1. Lester Charger Installed in SCT Electric Vehicle

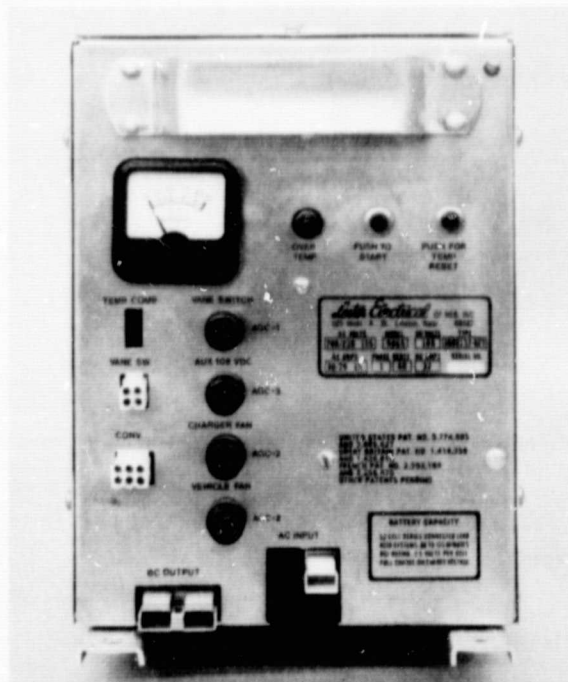


Figure 3-2. Front View of Lester Charger

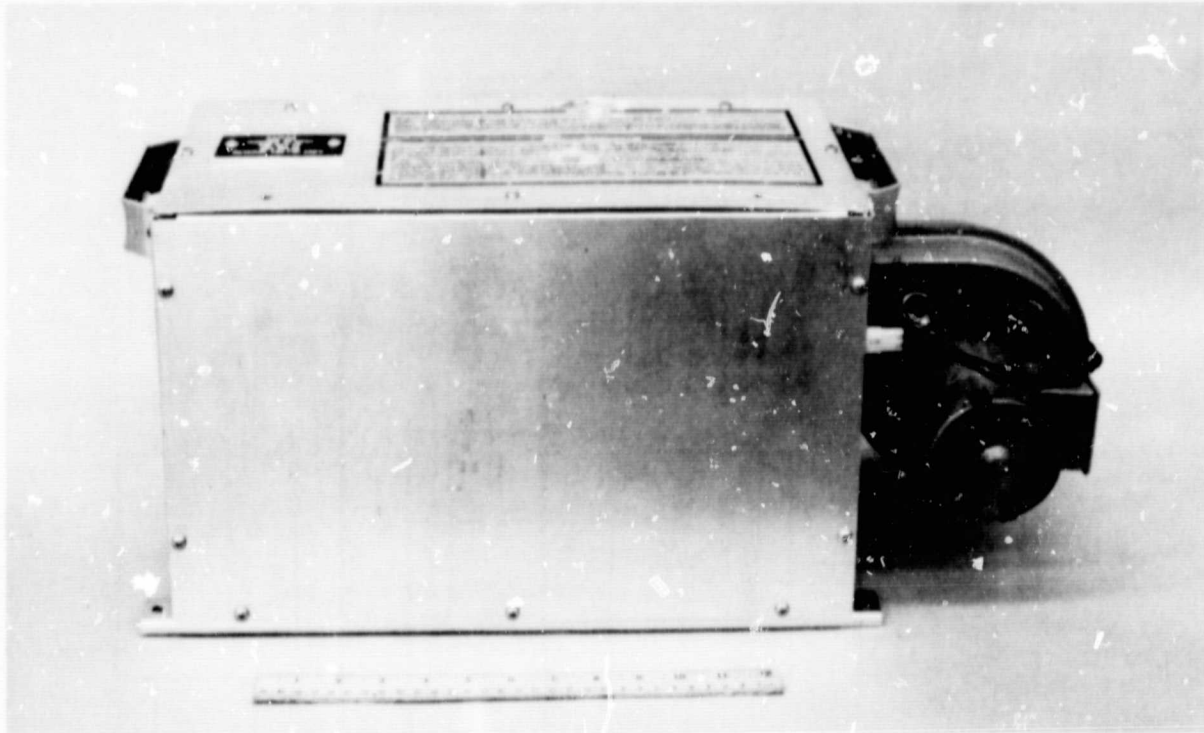


Figure 3-3. Side View of Lester Charger

of the charger (namely, charger shutdown) is not functional during 115-Vac operation. Isolation between the battery pack and the input powerline is also provided by this transformer. Battery charge current and voltage are controlled by silicon-controlled rectifiers (SCRs) in response to charge control logic that is proprietary to Lester. In addition to the basic charging function, the charger also controls a purge fan for the battery compartment. The purge fan is operated for 60 min following charge termination to ensure that hazardous gaseous effluents from the battery are purged from the battery compartment. Operation of the charger is interlocked with the purge fan as a safety feature. Charging cannot take place unless the fan is operating. Accessory battery charging is also done from the Lester charger. This is accomplished by supplying the dc-to-dc converter with power at 108 Vdc, as would be the case during vehicle operation. In this manner, the Lester charger is not required to duplicate the hardware already installed (e.g., dc-to-dc converter) for normal vehicle operation. Table 3-2 lists the charger electrical specifications.

#### C. CHARGE ALGORITHM

Operating instructions for the Lester charger provide little insight into its charge algorithm. Correspondence with Lester personnel provided the basis for the following description of the charge characteristics. When operated at the normal 208/230-Vac mode, and assuming the battery has been at least partially discharged, the following charge sequence occurs:

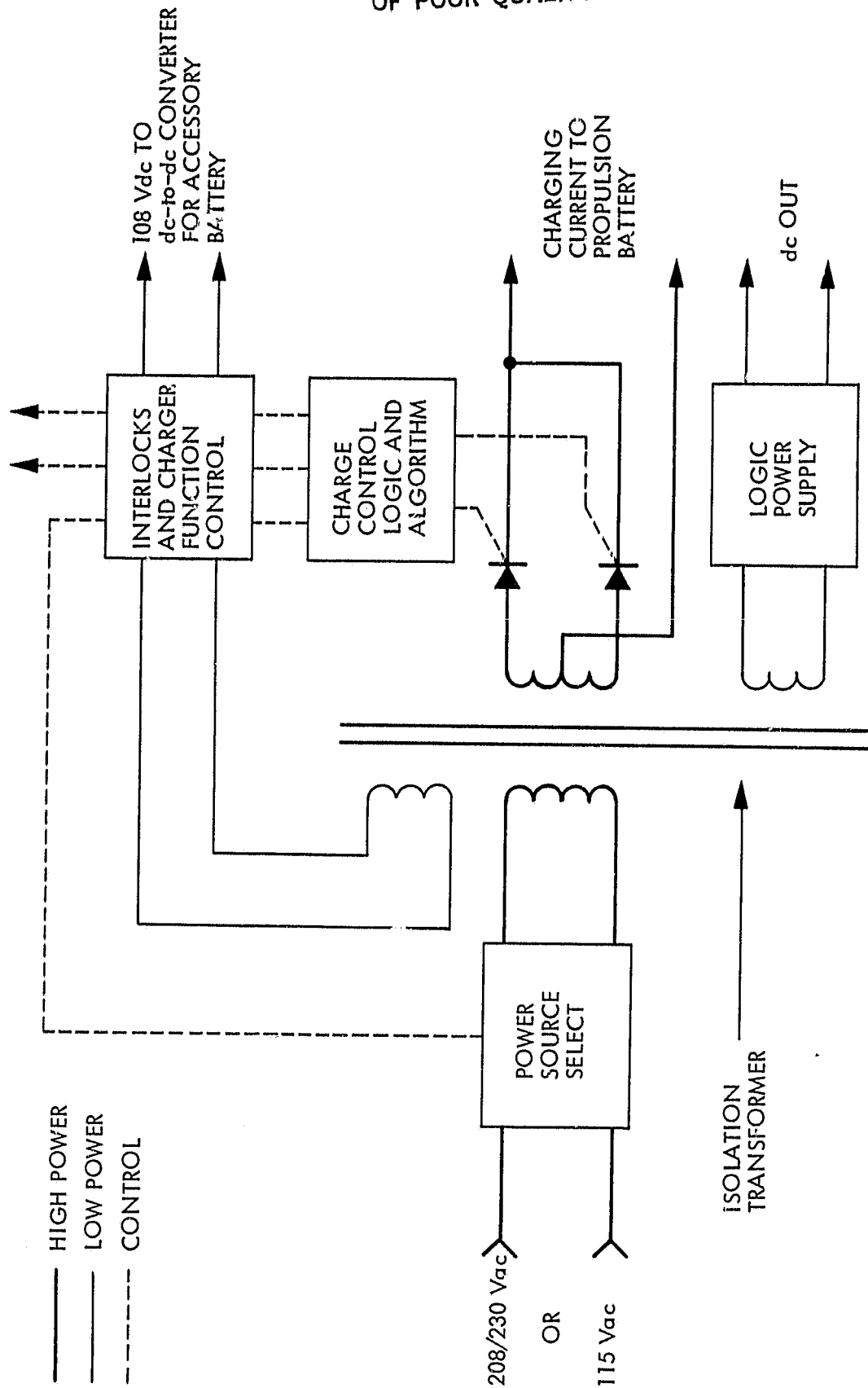


Figure 3-4. Block Diagram of Lester Charger



Table 3-2. Lester Charger Electrical Specifications

---

115 Vac-Mode	
Input Voltage	115 Vac
Input Current	15 A
Output Voltage	150 Vdc max
Output Current	8 Adc max
208/230-Vac Mode	
Input Voltage	208 or 230 <sup>a</sup> Vac
Input Current	25 A
Output Voltage	150 Vdc max
Output Current	32 Adc max

---

<sup>a</sup>Requires selection of appropriate tap on charger's input transformer.

---

- (1) Charge at a nominal fixed current of 32 A until battery voltage rises to 124 V (2.296 V/cell).
- (2) Decrease charge current linearly to approximately 8 A as battery voltage rises to 127.5 V (2.361 V/cell). In other words, from 124 to 127 V, battery current (32 to 8 A) is inversely proportional to battery voltage.
- (3) Maintain charge current at about 8 A until battery voltage rises less than 0.036 V (67  $\mu$ V/cell) in a 50-min period.
- (4) Terminate charge automatically.

Figure 3-5 shows the battery charger's voltage-current characteristic described above. From this figure it can be seen that, even when in the two constant current control modes (32 A or 8 A), there is a slight decrease in current as battery voltage increases. Lester consulted with ESB Company in the development of this charge algorithm. As such, some of the controlled parameters (e.g., 8-A finish current) reflect the needs of the XPV-23 battery, as defined by ESB. While the Lester's charge algorithm may not be the ultimate procedure, it is a considerable step in the right direction.

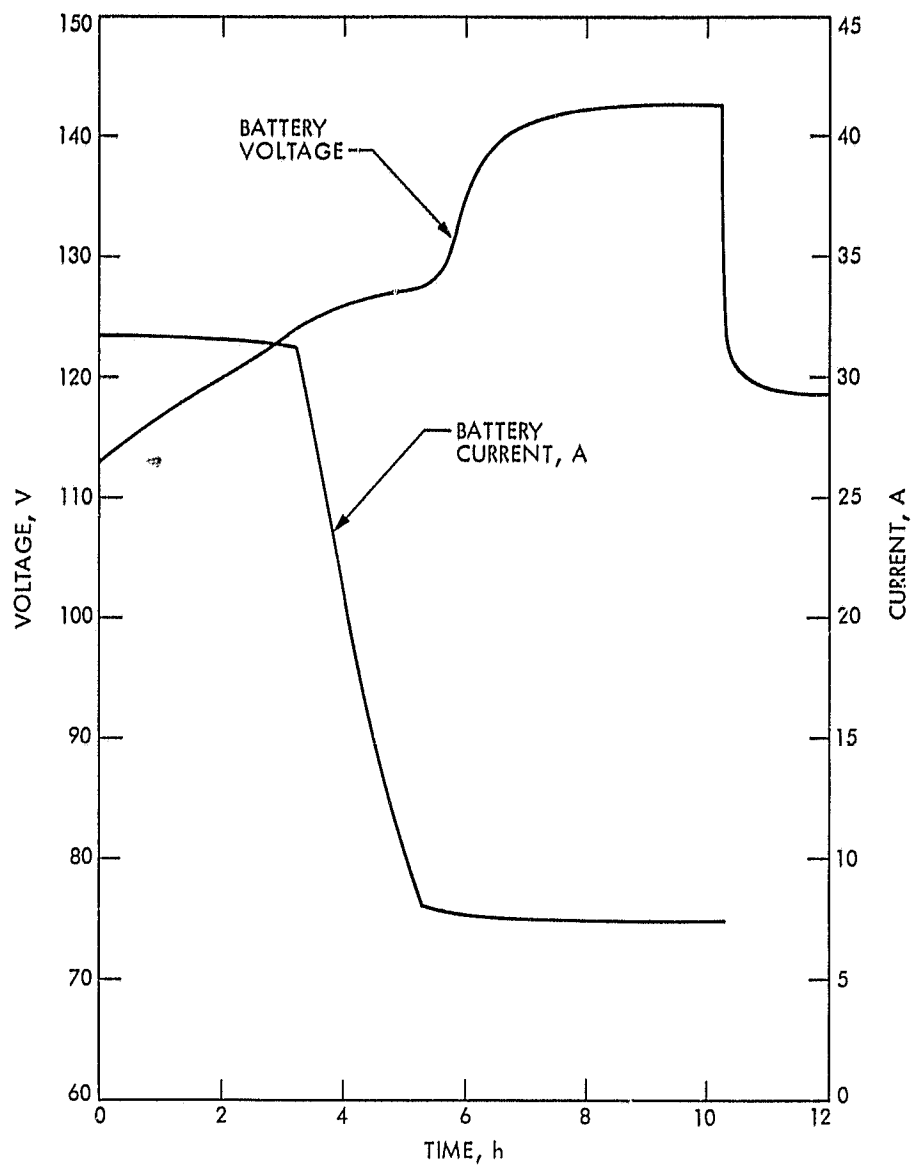


Figure 3-5. Voltage and Current Characteristics During Charge

## SECTION IV

### TEST PROGRAM AND METHODOLOGY

Ten charge/discharge cycle tests were performed at the JPL Automotive Research Facility from July 6 through July 23, 1981. The batteries were charged from various initial DoDs under the automatic control provided by the Lester charger. The batteries were then discharged to a prescribed level, based on initial capacity tests at a standard rate of 75 A in preparation for the next charge/discharge tests. Data from the charge/discharge tests were manually recorded, graphed on a real-time X-Y plotter and logged on a data acquisition system for later reduction. The data taken during charge included test number, date, initial DoD, charge time, battery terminal voltage, battery charging current, wall power, and temperatures at three locations in the battery pack. From these inputs, Integrated Data Acquisition and Control (IDAC) system data reduction computations gave outputs of battery charger efficiency, energy into the battery, energy into the charger, and battery ampere-hour (Ah) recharge values. Discharge data included battery discharge Ah, discharge energy, and estimated DoD.

The data for all tests are given in Appendix A and summarized in Table 4-1. The first column in the table shows the test number and date of the charge cycle, followed in the second column by the estimated DoD at the beginning of recharge. Values shown in the third, fourth, and fifth columns were taken from the real-time plots, showing times spent in each of the automatically controlled charge modes (high rate, taper, and finish) built into the charge logic, as well as the battery terminal voltage at the end of each mode. The sixth through tenth columns summarize Ah and energy data recorded during the charge and discharge cycles. The symbol definitions are as follows:

- ABO     = Amperage - Battery Out - (Discharge)  
          (Battery ampere hours extracted prior to the recharge cycle).
- ABIR    = Amperage - Battery In - Recharge  
          (Battery ampere hours supplied by the charger during recharge).
- EBO     = Energy - Battery Out (Discharge)  
          (Battery kilowatt hours extracted prior to the recharge cycle).
- EBIR    = Energy - Battery In - Recharge  
          (Battery kilowatt hours supplied by the charger during recharge).
- EBCIR   = Energy - Battery Charger In - Recharge (Wall)  
          (Wall-plug energy supplied to the charger at its input during the recharge cycle).

Columns 11 through 13 show battery and charger efficiencies calculated from the data recorded in Columns 6 through 10. The starting and ending temperatures at three locations in the battery pack are shown in the last two columns.

Table 4-1. Data Summary

Test No. and Date	Initial DoD, %	Charge-Mode Times (Mode Termination Volts)				Charge/Discharge Data					Efficiencies			Temperatures	
		High Rate	Taper	Finish	AB0	ABIR	EB0	EBIR	EBCIR	Ah	Wh	Charger Wh	Start	End	
11 7/6/81	100	3.2 (124)	2.1 (127)	4.9 (143)	151.25	75.96	--	22.56	27.64	85.96	--	81.61	84 85 85	104 113 105	
12 7/8/81	80	3.4 (124.5)	2.0 (127)	4.8 (143)	120.21	139.57	--	22.58	27.55	86.13	--	81.96	88 90 88	105 114 106	
13 7/9/81	60	2.5 (124)	1.9 (127)	3.7 (143)	91.57	108.79	--	18.04	21.97	84.17	--	82.11	91 99 94	105 115 105	
14 7/10/81	60	1.8 (124.5)	1.6 (127)	3.3 (144)	90.00	105.95	--	14.23	17.30	84.95	--	82.28	88 95 91	101 109 102	
15 7/13/81	40	1.7 (124.7)	1.7 (127+)	3.2 (145)	60.00	74.49	--	9.97	12.21	80.55	--	81.71	80 80 80	96 101 96	
16 <sup>a</sup> 7/14/81	20	0.8 (124.5)	1.5 (127+)	2.0 (145.5)	30.00	35.80 <sup>a</sup>	--	4.80	6.0 <sup>a</sup>	83.80 <sup>a</sup>	--	80.00 <sup>a</sup>	80 85 81	86 95 90	
18 7/17/81	80	2.6 (125)	1.7 (127)	4.2 (144)	120.00	141.93	--	18.39	22.50	84.55	--	81.74	84 91 86	102 111 102	
19 7/20/81	100	3.4 (124.5)	2.0 (127)	4.7 (143.5)	150.00	175.89	15.42	22.51	27.60	85.28	68.49	81.56	84 85 85	103 112 103	
20 7/22/81	40	1.0 (124.5)	1.3 (127)	3.1 (146)	60.00	76.54	6.32	10.19	12.50	78.39	62.03	81.48	79 81 79	95 99 95	
21 7/23/81	20	0.4 (125)	0.8 (127.5)	2.4 (147)	30.00	44.30	3.2	6.05	7.69	67.72	53.72	78.92	80 85 81	89 95 90	

<sup>a</sup>Charger terminated charging prematurely. Data is not representative.

Tests 18 through 21 were repetitions of Tests 11, 12, 15, and 16 and were made to verify the results of the earlier tests. During these tests, longer rest periods were allowed between charge and discharge to permit the batteries to reach more uniform temperatures.

## SECTION V

### DISCUSSION

ORIGINAL PAGE 19  
OF POOR QUALITY

Observations and analyses associated with the Lester charger tests are divided into three topics: the charge algorithm, charger efficiency, and charger waveshapes.

#### A. CHARGE ALGORITHM

The manner in which the charger operates with the battery is illustrated in Figure 5-1. The data shown in Figure 5-1 are reproduced from the original graphs taken during Test 11 for a complete recharge from 100% DoD. The characteristics displayed in the figure are typical of those obtained in all tests, regardless of the initial state of charge (SoC). These are best illustrated by the battery current and voltage traces (solid lines). During the initial high-rate charge period, the charger maintains a constant-charge current of 32 A. Battery voltage climbs from an initial value of 113 to 124 V during this mode.

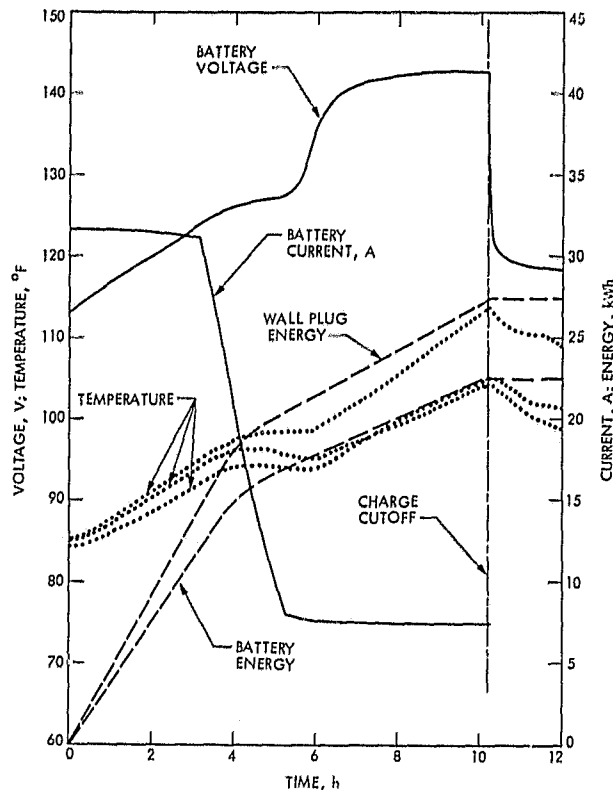


Figure 5-1. Battery Charge Profile for Test 11

The charger then proceeds into a taper mode in which the current decreases at a nearly linear rate. During this period the battery voltage rises slightly and then levels off at approximately 127 V at the end of the taper mode. At the conclusion of this period, the charge current has dropped to the finishing level of approximately 7.5 to 8 A and remains at this value throughout the finish charge period. During this mode, the battery terminal voltage climbs sharply to a value of 143 to 147 V, approaching this level asymptotically at final charge termination.

The operating instructions provided with the Lester charger do not describe the charge algorithm employed in its control. However, conversations with Lester personnel have clarified any areas of uncertainty. The following description of the charge algorithm is based on the conversations with Lester personnel, data from Columns 3 through 5 of Table 4-1, and the voltage and current traces of Figure 5-1:

- (1) High-rate charge-mode times vary with the initial SoC, as would be expected. However, the voltage at the termination of this mode varies only slightly from 124 to 125 V. This small variation might be attributed to measurement error or temperature effects in the charger. A slight drop off of the constant charge current can be seen in Figure 5-1. This current roll off was designed by Lester to increase the time spent in this high-current mode by delaying the onset of gassing.
- (2) During the taper mode, Figure 5-1 shows that the battery voltage rises to 127 V. As shown in Table 4-1, this mode termination voltage is common to all charges regardless of the initial SoC. However, Table 4-1 also shows that the taper mode time varies significantly as a function of initial state of charge. Thus, the rate of change-of-charge current with time varies as a function of initial battery state of charge. This is because the battery current is a function of battery voltage during the taper mode. As can be seen in Figure 5-2, battery current decreases from 32 to 8 A as battery voltage increases from 124 to 127 V. It has been JPL's experience that at the onset of gassing, battery voltage rises faster following shallow discharges. It is postulated that during shallow discharges, the individual cells have less opportunity to become unbalanced. As such, each cell approaches gassing potential in unison and battery voltage rises more rapidly.
- (3) The last mode of the charge is a constant 7.5 to 8 A. This current is maintained until the rise in battery voltage is less than 36 mV during a 50-min period. This relatively high finish current was specified by Exide to minimize electrolyte stratification. In other words, electrolyte mixing is achieved by the agitation associated with heavy gassing. It has been JPL's experience that the performance of the Exide battery is not compromised by a less strenuous finish current. The lower finish-charge current and reduced amount of overcharge previously reported by JPL had no discernable effect on battery performance (see Reference 2). It can therefore be reasonably postulated that both charge efficiency and battery life can be improved by a less strenuous charge.

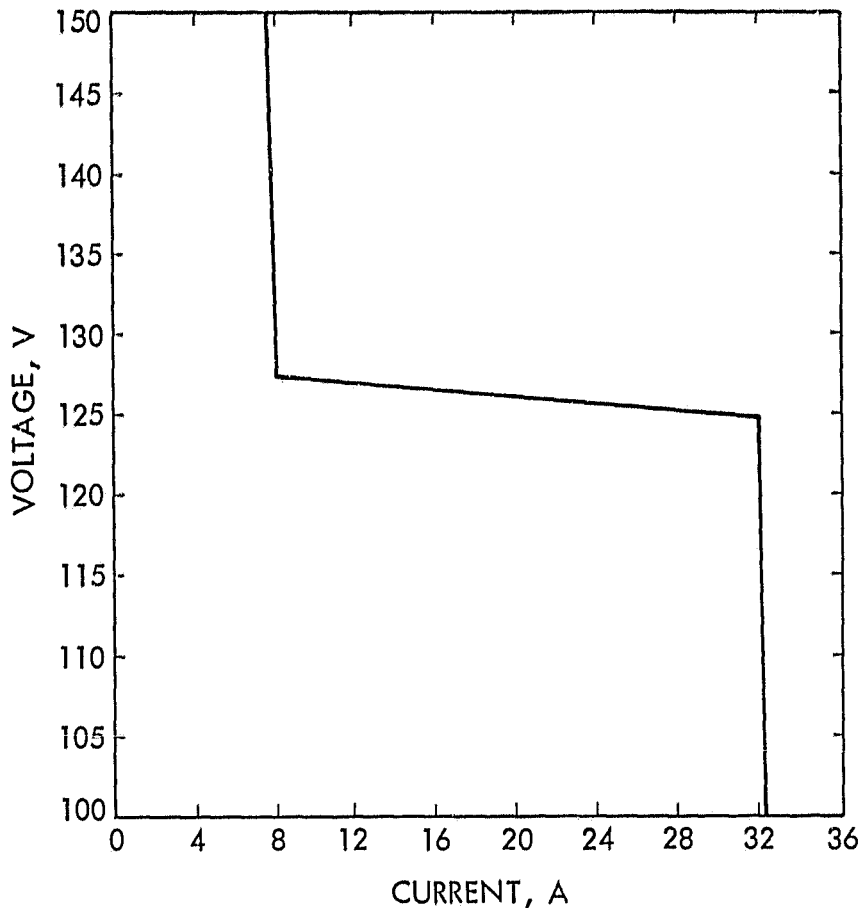


Figure 5-2. Charger Control Schedule (Source: Lester Electrical of Nebraska, Inc.)

As shown in Figure 5-1, battery voltage actually starts to decrease during the last half hour of charge. This is a result of the battery's voltage sensitivity to temperature. Prior to the last half hour, the battery's voltage sensitivity to SoC has been dominant, and any sensitivity to temperature is not readily discernible. Because the Lester charge algorithm does not account for temperature, it is possible that charging will be terminated due to the battery thermal environment rather than to the battery's charge needs. On the other hand, the possibility of thermal runaway is almost nonexistent. Any rise in battery temperature will result in a decrease in battery charge voltage and therefore contribute to the initiation of the termination criteria.

In the event that additional charge is desired after automatic shutdown, the controller can be reinitialized by interrupting power either by removing and replacing the power plug or by turning the main power switch off and on. On reapplication of power, the controller starts through a complete cycle, initially charging at the 32-A rate and then progressing into the taper and



finishing charge modes. Because the battery is already fully charged, the terminal voltage rises rapidly, causing the controller to transition quickly through the high-rate and taper-charge modes and into the finishing charge mode. Under this condition, the rate of change of voltage will be small, and the controller will proceed almost immediately into the 50-min shutdown sequence. Thus, by reinitializing the charger, an additional 50-min of over-charge at 7.5 to 8 A will be obtained before the charger again shuts down automatically.

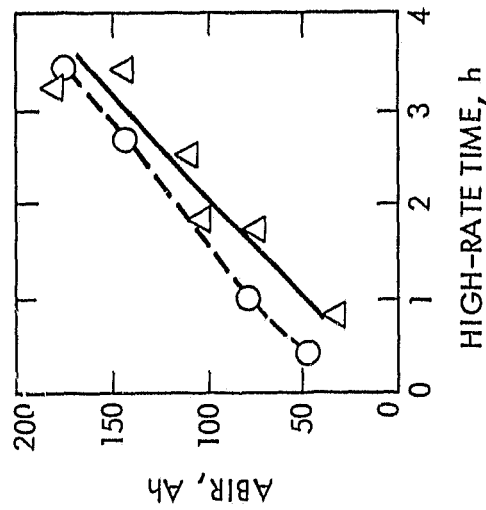
The curves of Figure 5-3 were plotted based on data in Columns 3, 4, and 5 of Table 4-1 for all tests. The solid-line curves represent data for the first test series (Tests 11 through 16), whereas the dashed-line curves apply to Tests 18 through 21. (It will be noted that the latter tests produced data points with less scatter.) In Figure 5-3(a), the high-rate charge time is plotted as a function of the total number of Ah applied throughout the entire charge schedule. The trend shows a generally linear relationship between the two with a slope of approximately 1 h of high-rate charge time for each 50 Ah of ultimate recharge. Thus, the time required to recharge to 124 V is closely representative of the initial DoD. In Figure 5-3(b), the taper-charge time is not directly related to the high-rate charge time, displaying an offset of approximately 1 to 1.5 h followed by a rather non-linear relationship to high-rate charge time. Similarly, Figure 5-3(c) shows the finishing rate time to have a 1 to 2 h offset before reflecting a near-linear relationship to the high-rate charge time. Interpretation of these curves is in general agreement with the information provided by Lester that the charge rates and termination criteria for the taper and finishing modes, respectively, are based on terminal voltage and the rate of change of terminal voltage.

## B. EFFICIENCIES

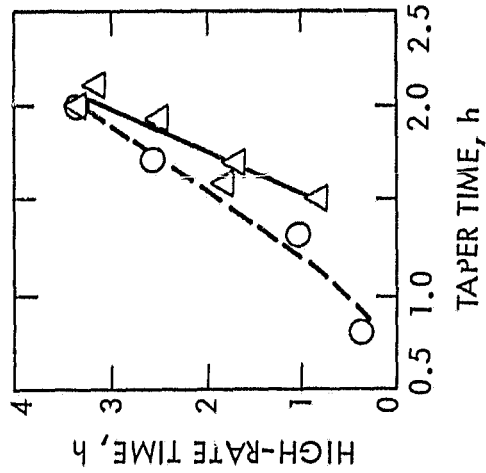
Figure 5-4 shows an IDAC plot of charger efficiency over a complete charge cycle with the battery initially at 100% DoD. Superimposed on the efficiency graph are curves of battery voltage and charge current. Dependencies of charger efficiency on load voltage and current are discernible in the plots, as evidenced by the rise in efficiency as the battery terminal voltage climbs during the high-rate and early taper-charge modes and by the decline in efficiency as the current falls below approximately 23 A during the taper and finishing-charge modes. The sensitivity of efficiency to battery voltage is also evident during the finishing-charge mode when the charger efficiency increases slightly along with the slight rise in terminal voltage. An exception to these observations will be noted at the beginning of charge when the charger efficiency decreases slightly even as the battery voltage is increasing. This may be due to a thermal effect in the charger circuitry during the initial warm-up period.

These dependencies are illustrated more clearly in the plots of Figure 5-5. Figure 5-5(a) shows the direct effect of battery voltage on charger efficiency at the high-rate current setting (31 to 32 A) and finishing rate (7.5 A), and also indicates the inverse relationship between efficiency and load current. It will be noted that the sensitivity of efficiency to voltage is greater at high-load currents than at low-load currents. Using the two

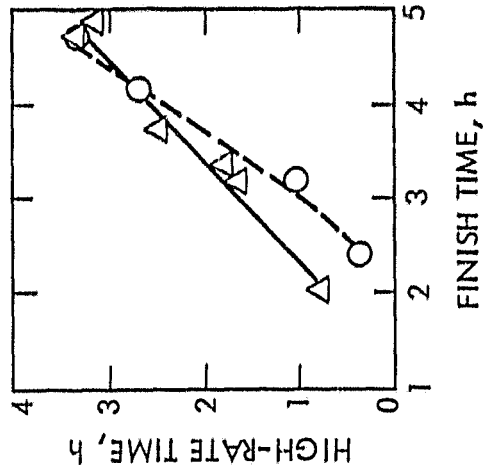
○--- TESTS 17 THROUGH 16  
△--- TESTS 18 THROUGH 21



(a) HIGH-RATE MODE TIME vs. ABIR



(b) TAPER MODE TIME vs. HIGH-RATE TIME



(c) FINISH MODE TIME vs. HIGH-RATE TIME

Figure 5-3. Charge-Mode Times

currents as a base and assuming that a linear dependence exists between charger efficiency and load current, the sensitivity of charger efficiency to load current can be calculated as  $-0.23\%/A$ . The individual effects of load current are somewhat obscured in the curve of Figure 5-5(b), which is a plot of charger efficiency as a function of battery charge power.

Figure 5-6 shows the net effects of these parameters on average battery and charger efficiencies for all tests. These curves cover the range of initial DoD states from 20 to 100%. As in Figure 5-3, the solid-line plots represent data from the first test series (Tests 11 through 16) whereas the dashed line curves are for Tests 18 through 21. The battery Ah efficiency curves of Figure 5-6(a) show the combined effects of battery coulombic efficiency and overcharging on overall battery charge discharge efficiency. Because an optimally charged lead-acid cell will normally exhibit a coulombic efficiency of 97 to 99% (Reference 3), most of the Ah efficiency degradation represented by the curves of Figure 5-6(a) is interpreted as the effects of

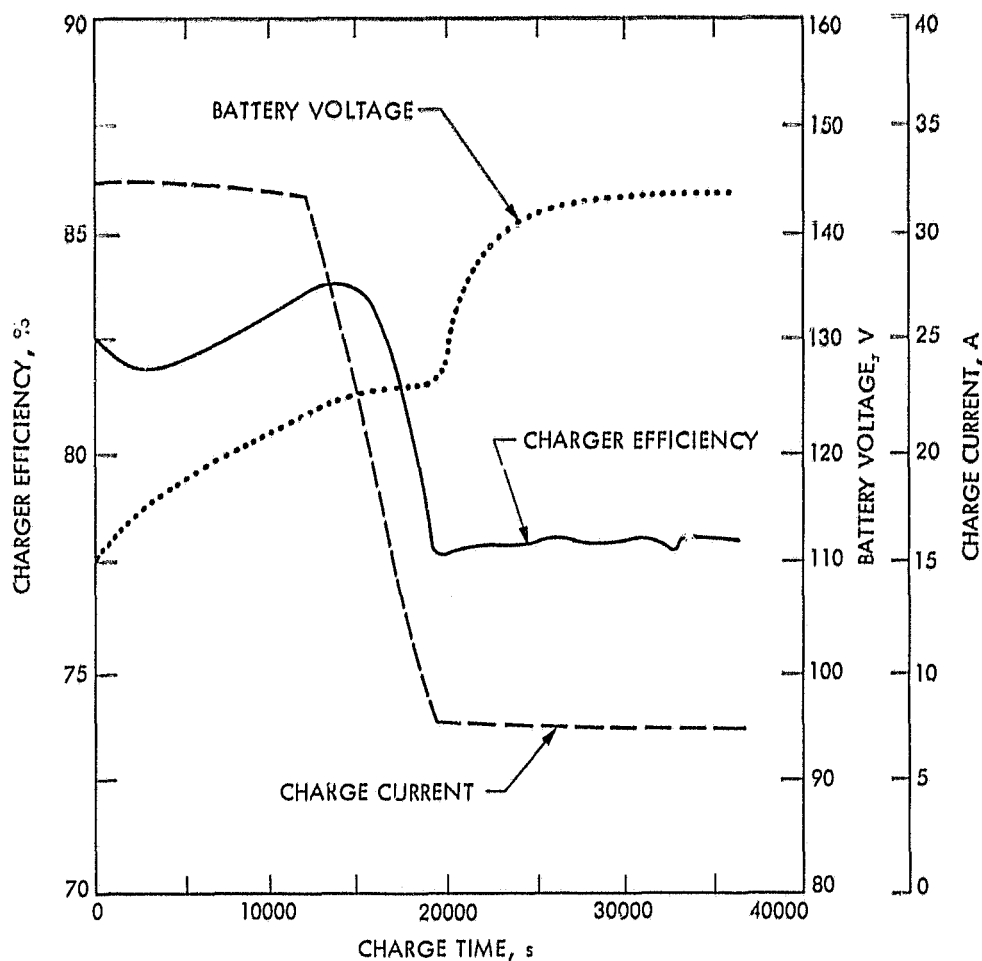
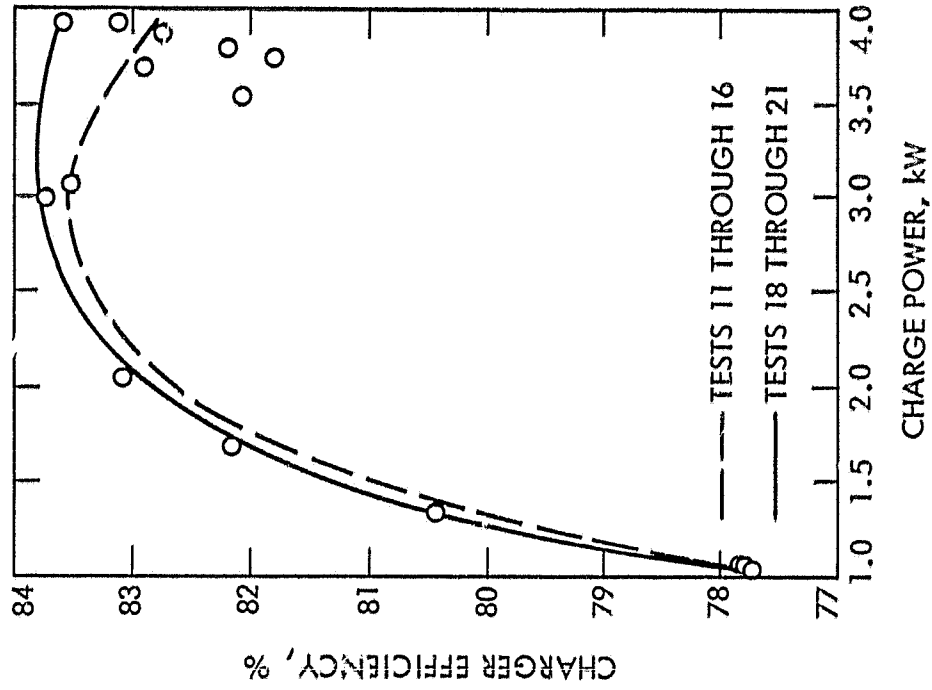
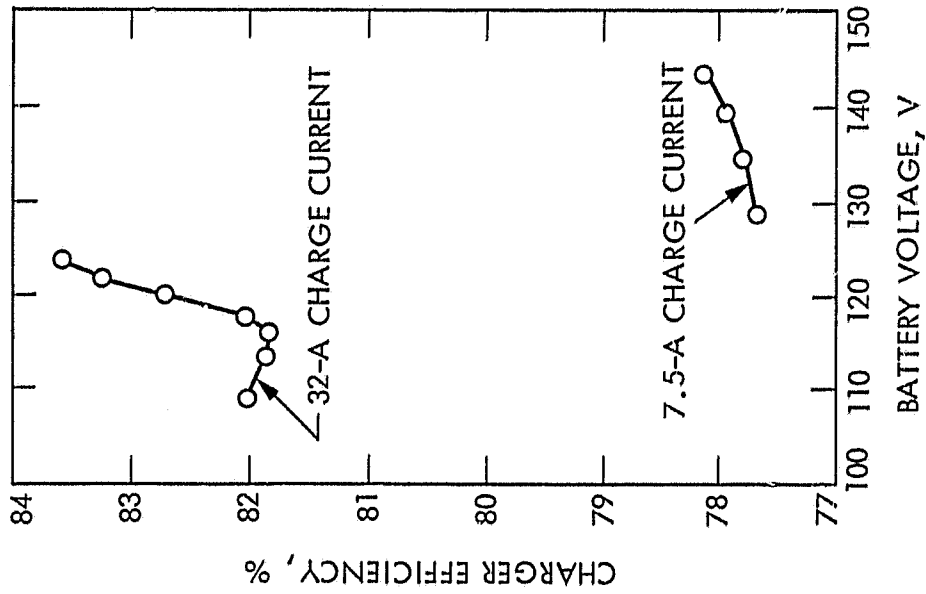


Figure 5-4. Instantaneous Charger Efficiency During Typical Charge Cycle (Test No. 19)



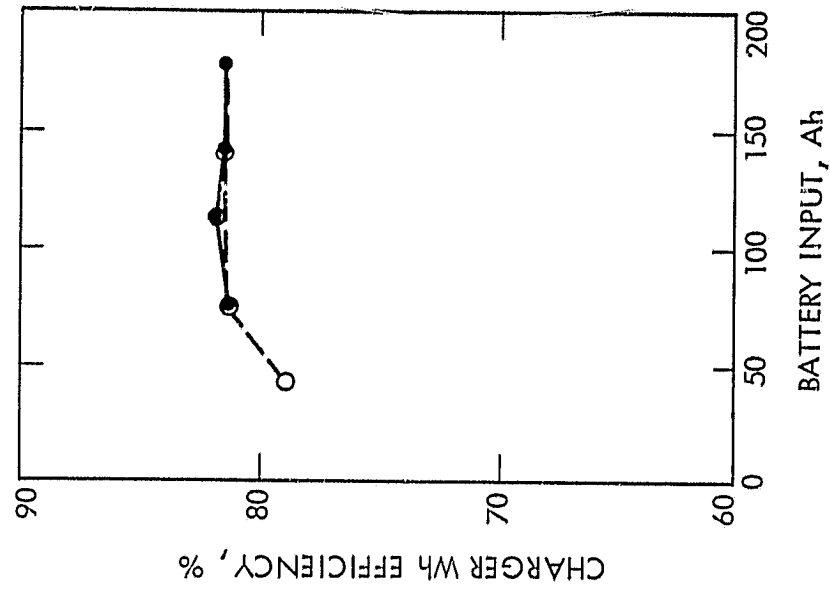
(b) SENSITIVITY OF CHARGER  
EFFICIENCY TO CHARGE  
POWER



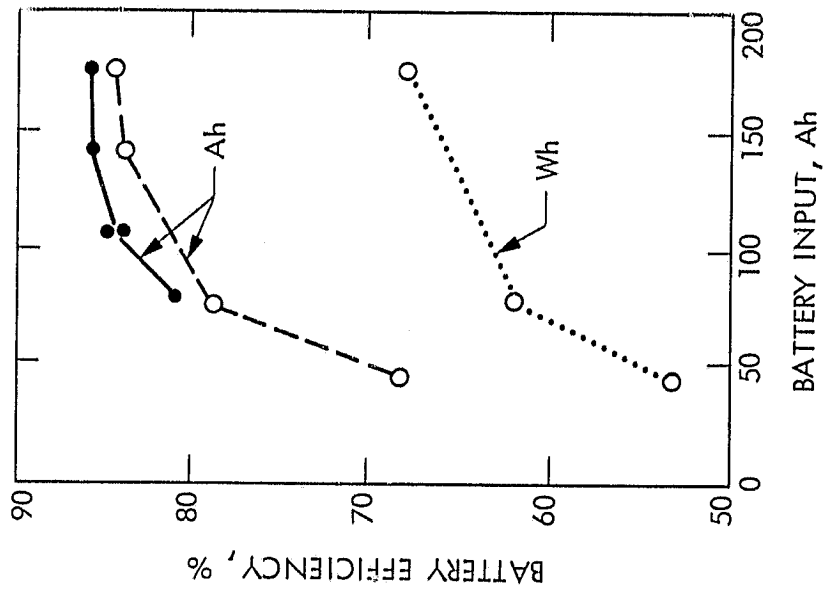
(a) SENSITIVITY OF CHARGER  
EFFICIENCY TO BATTERY  
VOLTAGE

Figure 5-5. Instantaneous Charger Efficiency

ORIGINAL PAGE IS  
OF POOR QUALITY



(b) CHARGER ENERGY EFFICIENCY  
(CHARGE ONLY)



(a) BATTERY EFFICIENCY  
(CHARGE/DISCHARGE)

Figure 5-6. Battery/Charger Efficiencies

overcharge. Overcharging serves two purposes in a multi-battery string: (1) to ensure that the weaker cells are brought up to a full SoC each recharge and (2) to reduce electrolyte stratification by agitation produced in the gas evolution process. Although the curves show a reasonable degree of overcharge when the batteries are fully charged from a heavily discharged initial state, the degree of overcharge for only lightly discharged batteries appears to be excessive. The battery Watt-hour (Wh) efficiency, graphed in the lower portion of Figure 5-6(a), is based on data for only three measurements made during Tests 19, 20, and 21. This curve appears to be consistent with expectations, considering the extent of overcharge evidenced by the Ah efficiency curves. Individual lead-acid batteries normally exhibit Wh efficiencies from 80 to 85% when optimally charged (Reference 3). These data would indicate optimum Wh efficiencies from 75 to 80% when adjusted for overcharge effects needed to avoid stratification in multi-battery strings.

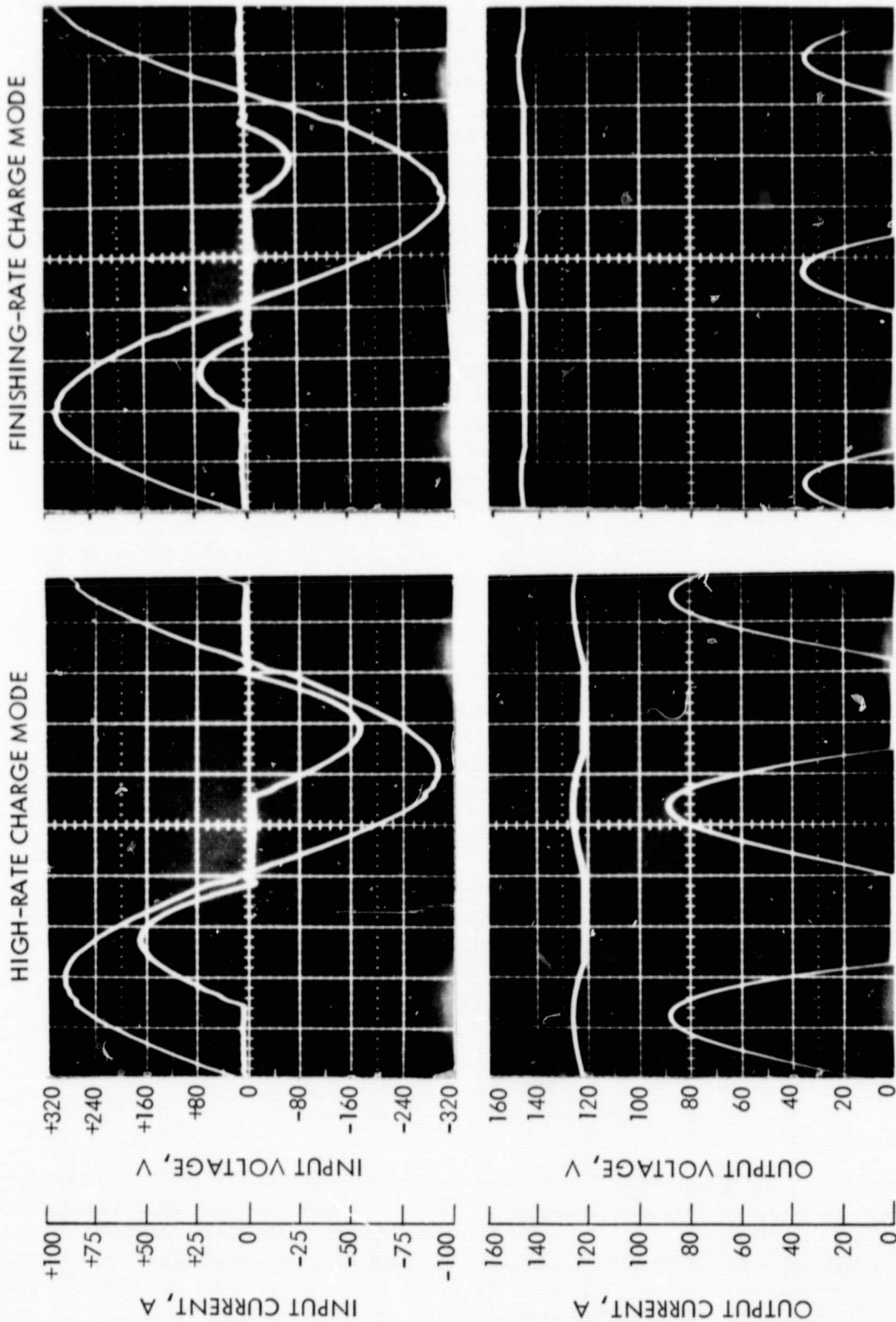
Charge-cycle energy efficiencies of the charger for charges ranging from 20 to 100% of the maximum battery capacity are shown in Figure 5-6(b). These curves integrate the instantaneous effects of load current and voltage on charger efficiency throughout complete charge cycles. This figure shows that the net charger efficiency is relatively independent of initial battery SoC, indicating only a slight degradation in overall efficiency for very light charges. This effect is probably due to the fact that the lower efficiency finishing charge rate represents a larger fraction of the total charge energy during light charges.

### C. CHARGER WAVEFORMS

Typical input and output voltage and current waveforms are shown in Figure 5-7 for charger operation in the high- and finishing-rate charge modes. The high-rate charge oscilloscope photographs were taken at approximately the 60% DoD level after a 20% recharge following an 80% discharge. The finishing-rate charge traces were obtained at nearly the 100% state of charge level after an 80% recharge following an 80% discharge. The phase lag, asymmetrical leading and trailing slopes, and turnoff overshoot observed in the input-current waveforms are indicative of an inductive-load component, resulting from the relatively high leakage reactance and/or poor coupling in the charger's isolation transformer. The fact that there are no other reactive components shown in the manufacturer's circuit diagram (Appendix A) and their statement that the transformer's gap was increased<sup>1</sup> supports the aforementioned hypothesis. The transients observed in the input voltage

---

<sup>1</sup>Lester personnel indicated that the gap between the isolation transformer windings was increased for two reasons: (1) to effect a current limit by decreasing the coupling and (2) to enhance the ability to vary voltage over the range needed to accommodate electrolyte temperature compensation. Temperature compensation was not included in JPL's charger due to delivery time constraints to the vehicle manufacturer.



(a) HIGH-RATE CHARGE MODE VOLTAGE AND CURRENT WAVEFORMS

(b) FINISHING-RATE CHARGE MODE VOLTAGE AND CURRENT WAVEFORMS

Figure 5-7. Lester Charger Input and Output Voltage and Current Waveforms

waveform at current turn on could be a cause of conducted or local radiated noise in the vicinity of the charger. The frequency of the transient is approximately 2000 Hz, and it decays in two to three cycles.

The output voltage waveform in the high-rate charge mode shows about a 5-V instantaneous excursion at the peak current of 90 A, indicating that the battery internal resistance at this level is approximately 55 m $\Omega$ . The average battery terminal voltage at this SoC is 122 V at an average dc charge current of approximately 30 A. The current waveform is characterized by asymmetrical leading and trailing slopes indicative of an inductive source; and, as would be expected, there are no transients in the turn-off region. The output traces of the finishing-rate charge mode are predictable, showing a shorter current-conduction angle, lower peak current, and a higher battery-terminal voltage that is approximately 143 V at the 8-A charge rate. The coarse resolution of the traces does not permit a reasonable estimate of the battery internal resistance at this lower charging current.

Except for different voltage and current levels, oscilloscope traces taken during the taper charge mode were consistent with those shown in Figure 5-7 for the high-rate and finishing-rate charge modes. Additional oscilloscope traces are provided in Appendix A.



## SECTION VI

### CONCLUSIONS AND RECOMMENDATIONS

#### A. CONCLUSIONS

The Lester charger performed well and consistently during testing. After an initial failure problem, which was quickly repaired by Lester, the charger operated reliably for more than 2 years. The following conclusions were derived from this test program:

- (1) Although the Lester charge algorithm could not be considered "sophisticated," it is a considerable improvement over any commercially available charge controls known to the authors to date.
- (2) The charger itself is reasonably efficient. Although other, more efficient, chargers are commercially available, their lack of a precise charge algorithm can result in a much poorer overall battery/charger efficiency. Overall efficiency from the "wall" is determined by the product of charger and battery throughput efficiency. Therefore, both must be considered when evaluating charger efficiency.
- (3) During conditions of shallow discharge, the combined charger and battery efficiencies decrease because of the fixed, 50-min period at the end of charge. In other words, charger and battery throughput efficiency would both be enhanced if the period of the finish charge was a function of DoD when charge is initiated.
- (4) The lack of electrolyte temperature compensation will impair the quality and efficiency of recharge when battery temperature deviates from the nominal 27°C (80°F) for which the charge algorithm was developed. It is postulated that, when temperature is above approximately 46°C (115°F), battery voltage will not rise to the 124-V lid at which current tapering is initiated. Therefore, charging would continue at the high 32-A rate until the dv/dt charge termination criterion is satisfied. The opposite problem will occur at colder battery temperatures. The charger will sense a higher voltage prematurely and go to the low-current charge earlier than required. Both of these temperature-related charging problems are detrimental to the battery's life and/or performance.
- (5) The technique of reducing the isolation transformer's flux by increasing the winding gap is an inefficient method to achieve current limiting.

#### B. RECOMMENDATIONS

The objectives of the test program were not fully satisfied because the effect of battery temperature on battery charge/discharge and charger effi-

iciency was not investigated. However, the following recommendations are valid until additional testing, at different temperatures, proves otherwise:

- (1) Charge algorithms, specifically for lead-acid batteries, must compensate for battery temperature unless their temperature is controlled to a specific value. Unless recharge is compensated, the battery would probably be overcharged or undercharged. In either case, battery performance, life, and/or maintainance will suffer.
- (2) Some charging testing should be performed at elevated and reduced battery temperatures to quantify the severity of the problem for this particular charge algorithm.
- (3) Lester could investigate an improved design for the charger's isolation transformer. The coupling efficiency and power factor can both be enhanced, thereby improving charger throughput efficiency.
- (4) In general, the whole area of battery charging needs more attention. Improper charging (e.g., no temperature compensation, etc.) appears to be one of the larger parameters causing the battery problems witnessed by the EV site operators (i.e., short battery life and excessive maintenance), yet little is being done to remedy the problem(s). For instance, Lester's early attempt to include temperature compensation was frustrated by a lack of data from the battery manufacturer. Even though the charger discussed in this report represents some answers to the charging problems, much remains to be done. Considering the relative benefits of developing improved charge algorithms versus the cost of development, charge algorithm development would be a cost-effective and worthwhile effort.

## REFERENCES

1. Edwards, D., On-Board Battery Charger/State of Charge Indicator, JPL Report 5030-514, Jet Propulsion Laboratory, Pasadena, California, December 1981.
2. Bryant, J., et al., Upgraded Demonstration Vehicle Task Report, JPL Publication 81-98, Jet Propulsion Laboratory, Pasadena, California, October 15, 1981.
3. Rowlette, J., Electric and Hybrid Vehicles Charge Efficiency Tests of ESB EV-106 Lead-Acid Batteries, JPL Publication 80-94, Jet Propulsion Laboratory, Pasadena, California, January 15, 1981.

# APPENDIX A

## DATA SUMMARY OF TESTS ON THE LESTER CHARGER WITH EXIDE BATTERIES

### 7/14/81 - Charge Cycle No. 11 - 100% DoD

$\frac{ABO}{ABIR}$	$\frac{151.25}{175.96}$	85.96% Battery Efficiency
--------------------	-------------------------	---------------------------

$\frac{EBIR}{EBCIR}$	$\frac{22.562}{27.638}$	81.61% Charger Efficiency
----------------------	-------------------------	---------------------------

Battery Temperatures - 84°, 85°, 85° at start of charge  
- 104°, 113°, 105° at end of charge

### 7/14/81 - Charge Cycle No. 12 - 80% DoD

$\frac{ABO}{ABIR}$	$\frac{120.21}{139.57}$	86.13% Battery Efficiency
--------------------	-------------------------	---------------------------

$\frac{EBIR}{EBCIR}$	$\frac{22.582}{27.553}$	81.96% Charger Efficiency
----------------------	-------------------------	---------------------------

Battery Temperatures - 88°, 90°, 85° at start of charge  
- 105°, 114°, 106° at end of charge

### 7/14/81 - Charge Cycle No. 13 - 60% DoD

$\frac{ABO}{ABIR}$	$\frac{91.57}{108.79}$	86.13% Battery Efficiency
--------------------	------------------------	---------------------------

$\frac{EBIR}{EBCIR}$	$\frac{18.037}{21.966}$	82.1% Charger Efficiency
----------------------	-------------------------	--------------------------

Battery Temperatures - 91°, 99°, 94° at start of charge  
- 105°, 115°, 105° at end of charge

### 7/14/81 - Charge Cycle No. 14 - 60% DoD

$\frac{ABO}{ABIR}$	$\frac{90.00}{105.95}$	84.95% Battery Efficiency
--------------------	------------------------	---------------------------

$\frac{EBIR}{EBCIR}$	$\frac{14.232}{17.298}$	82.28% Charger Efficiency
----------------------	-------------------------	---------------------------

Battery Temperatures - 88°, 95°, 91° at start of charge  
- 101°, 109°, 102° at end of charge

# DATA SUMMARY (Cont'd.)

## 7/14/81 - Charge Cycle No. 15 - 40% DoD

ABO	60.00	80.55% Battery Efficiency
ABIR	<u>74.49</u>	

EBIR	9.973	81.71% Charger Efficiency
EBCIR	<u>12.206</u>	

Battery Temperatures - 80°, 80°, 80° at start of charge  
 - 96°, 101°, 96° at end of charge

## 7/14/81 - Charge Cycle No. 16 - 20% DoD

ABO	30.00	83.80% Battery Efficiency
ABIR	<u>35.80</u>	

EBIR	4.80	80.00% Charger Efficiency
EBCIR	<u>6.00</u>	

Battery Temperatures - 80°, 85°, 81° at start of charge  
 - 88°, 95°, 90° at end of charge

## 7/14/81 - Discharge #17, Charge #18 - 80% DoD<sup>1</sup>

ABO	120.00	84.55% Battery Efficiency
ABIR	<u>141.93</u>	

EBIR	18.390	81.74% Charger Efficiency
EBCIR	<u>22.499</u>	

Battery Temperatures - 84°, 91°, 86° at start of charge  
 102°, 111°, 102° at end of charge

## 7/21/81 - Discharge #17, Charge #19 - 100% DoD

ABO	150.00	85.28% Battery Efficiency
ABIR	<u>175.89</u>	

EBIR	22.510	81.56% Charger Efficiency
EBCIR	<u>27.601</u>	

EBO	15.418	68.49% Battery Energy Efficiency
EBIR	<u>22.510</u>	

Battery Temperatures - 84°, 85°, 85° at start of charge  
 103°, 112°, 103° at end of charge

---

<sup>1</sup>Note: Charger terminated charging prematurely.

# DATA SUMMARY (Cont'd.)

## 7/22/81 - Discharge #19, Charge #20 - 40% DoD

ABO	60.00	78.39% Battery Efficiency
ABIR	<u>76.54</u>	

EBIR	10.187	81.48% Charger Efficiency
EBCIR	<u>12.502</u>	

EBO	6.320	62.03% Battery Energy Efficiency
EBIR	<u>10.189</u>	

Battery Temperatures - 78°, 81°, 79° at start of charge  
95°, 99°, 95° at end of charge

## 7/22/81 - Discharge #20, Charge #21 - 20% DoD

ABO	30.00	67.72% Battery Efficiency
ABIR	<u>44.30</u>	

EBIR	6.050	78.92% Charger Efficiency
EBCIR	<u>7.666</u>	

EBO	3.25	53.72% Battery Energy Efficiency
EBIR	<u>6.05</u>	

Battery Temperatures - 80°, 85°, 81° at start of charge  
89°, 95°, 90° at end of charge

# APPENDIX B

## CALCULATED DATA: CHARGER AND BATTERY THROUGHPUT EFFICIENCIES

Table B-1. Data Log Summary: Recharge Efficiencies from Various Depths of Discharge

Depth of Discharge, %	Charger Energy Efficiency, %	Battery Throughput Efficiency, %
100	81.60	85.96
80	81.96	86.13
60	82.11	84.17
40	81.71	80.55
20	78.92	67.72

APPENDIX C

CHARGER/BATTERY RECHARGE CHARACTERISTICS  
FOR SEVERAL TESTS

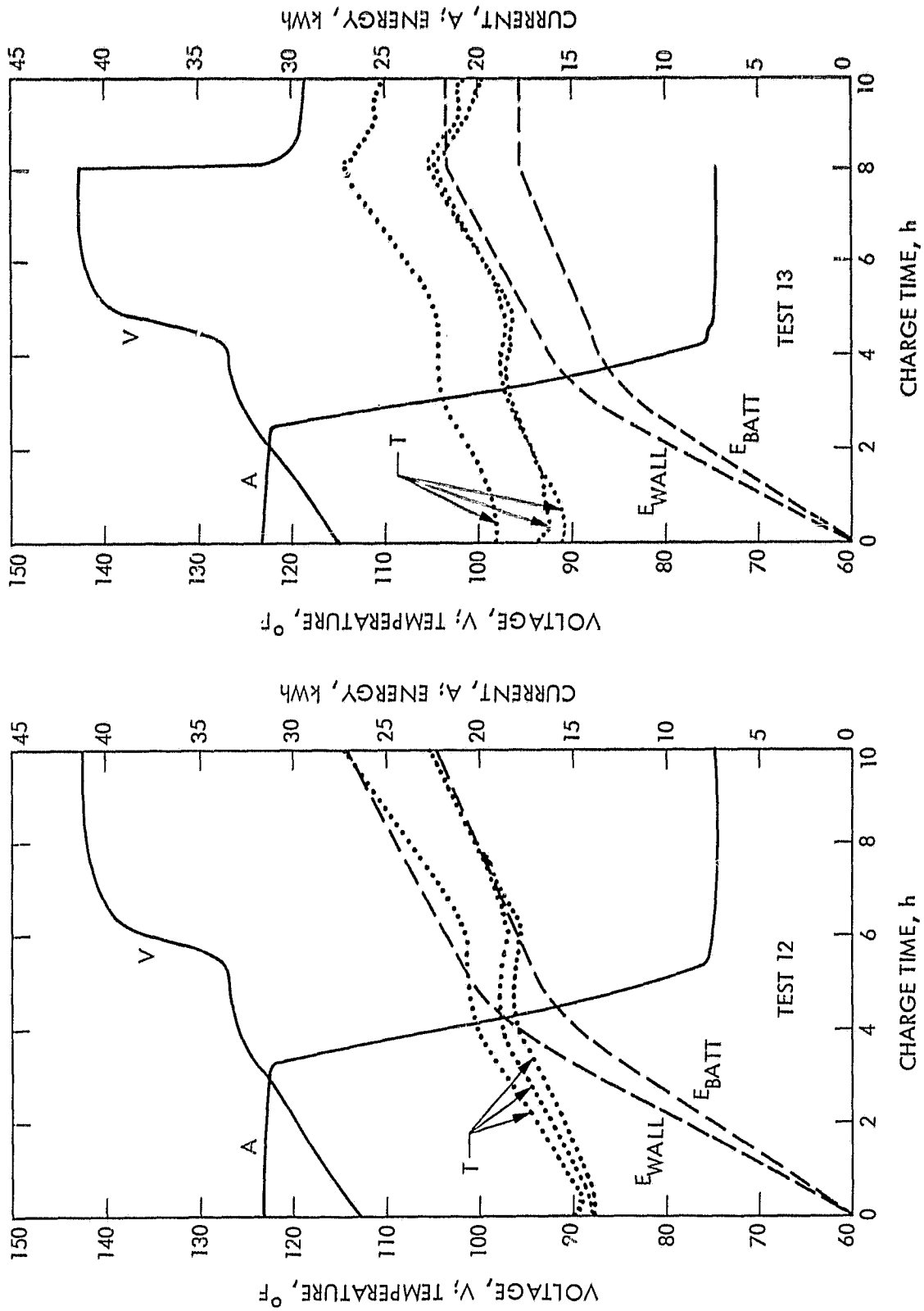


Figure C-1. Charge Characteristics for Tests 12 and 13



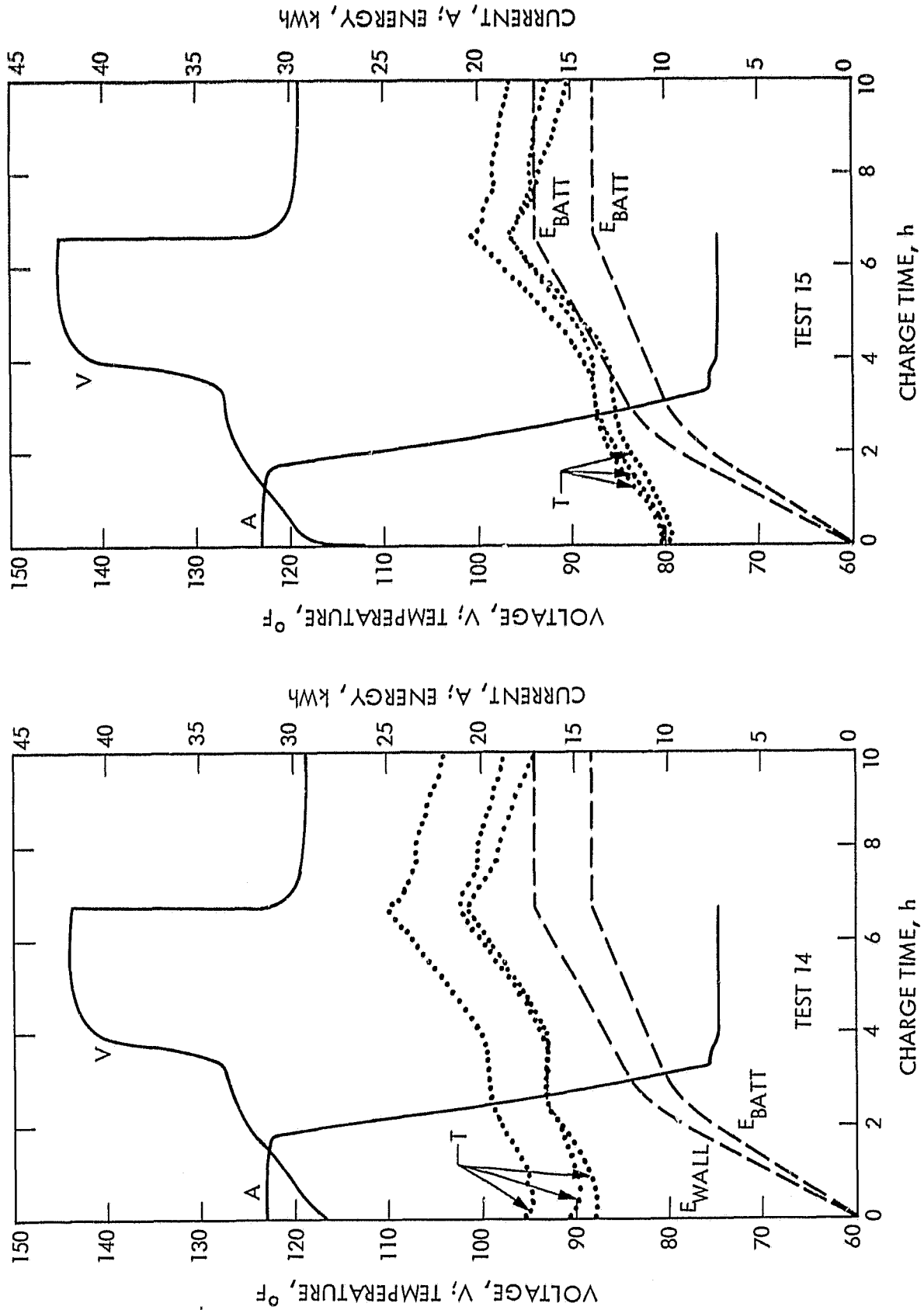


Figure C-2. Charge Characteristics for Tests 14 and 15

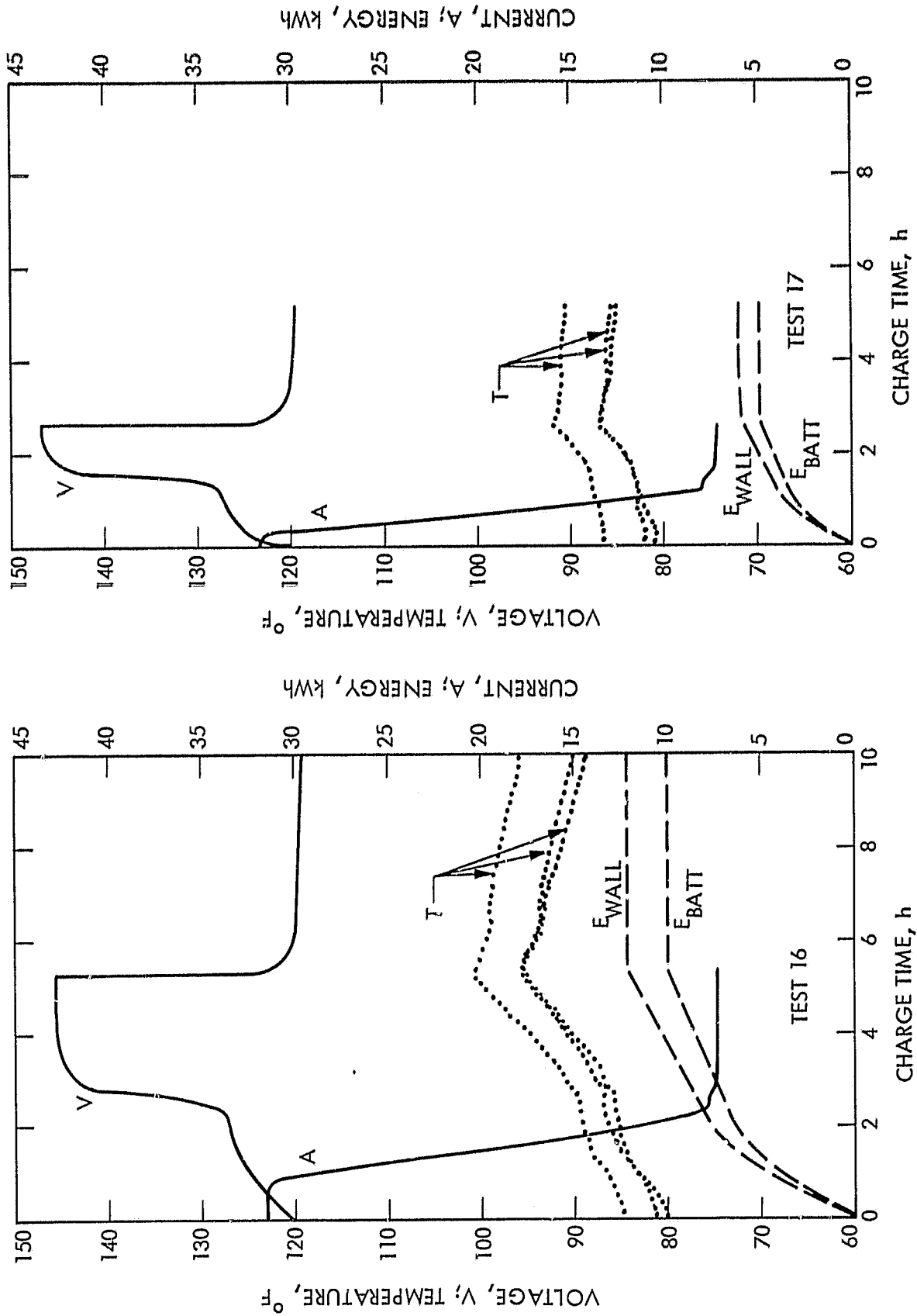


Figure C-3. Charge Characteristics for Tests 16 and 17

APPENDIX D

TYPICAL OSCILLOGRAPHS OF CHARGER INPUT AND OUTPUT  
POWER VS. AMPERE-HOUR CHARGES

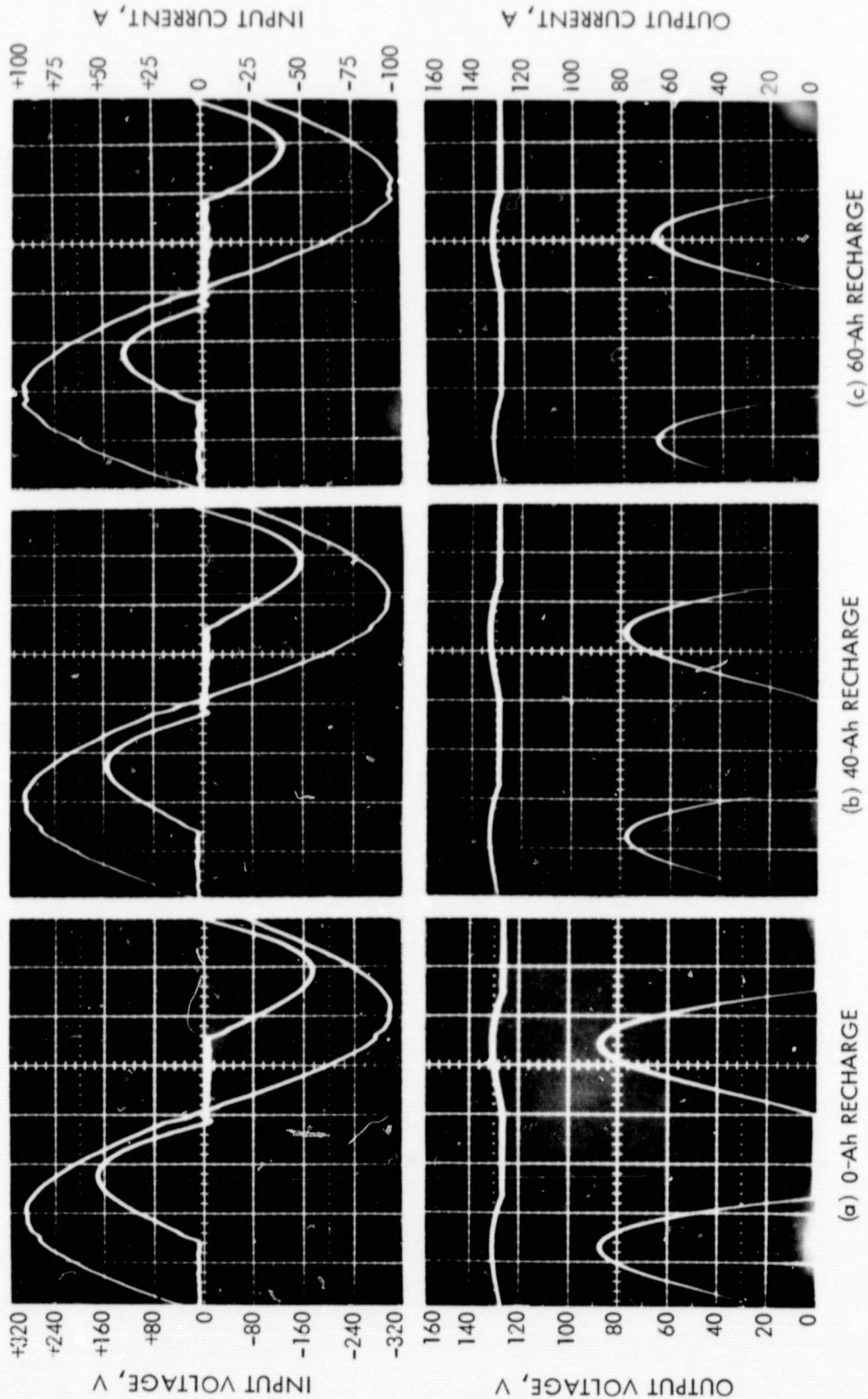


Figure D-1. Oscillographs of Charger Input and Output Waveforms for Test 12 at (a) 0- (b) 40- (c) 60-Ah Recharge

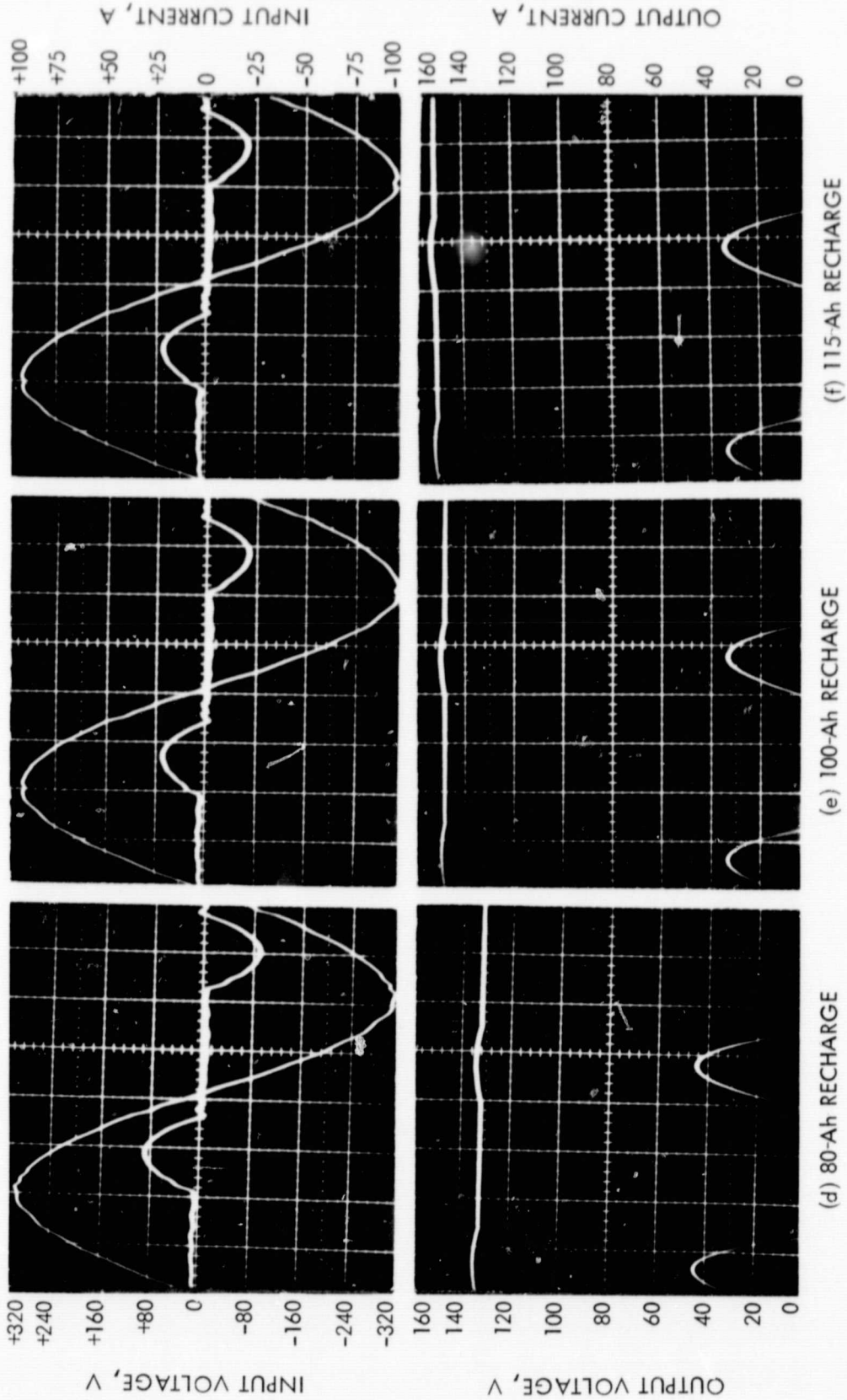
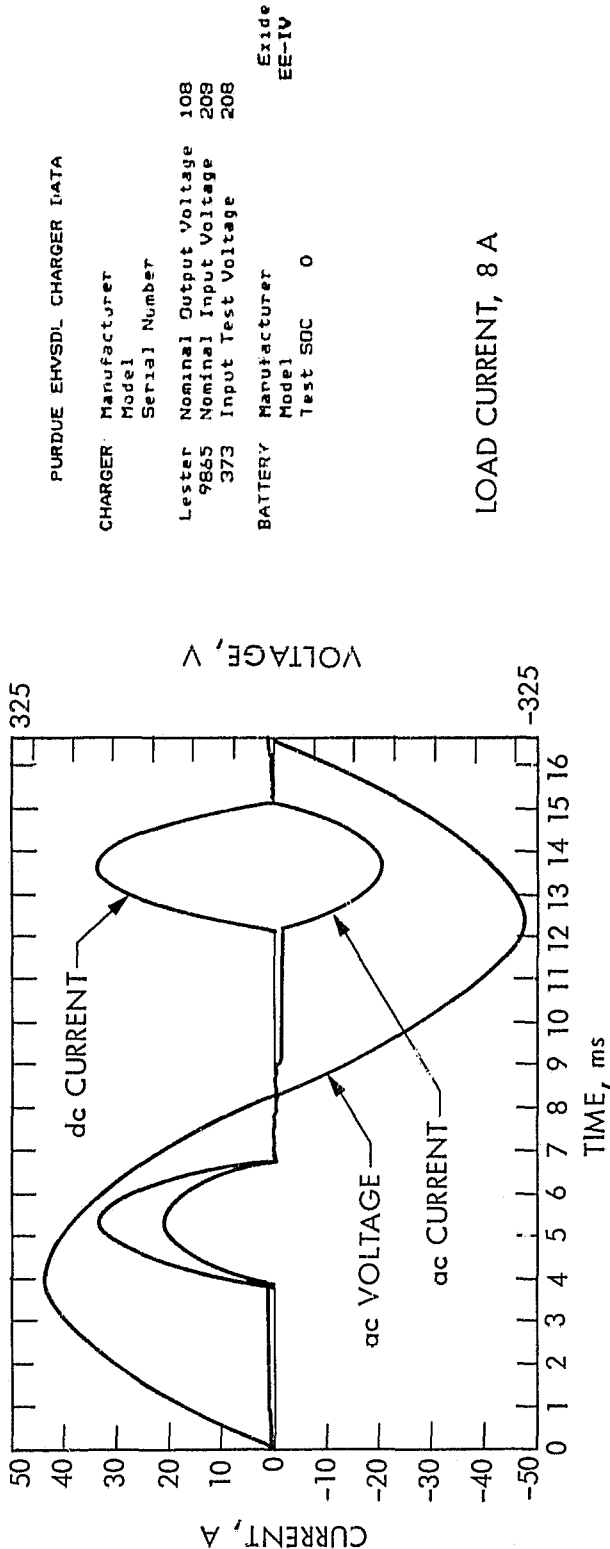


Figure D-2. Oscillographs of Charger Input and Output Waveforms for Test 12 at (d) 80- (e) 100- (f) 115-Ah Recharge

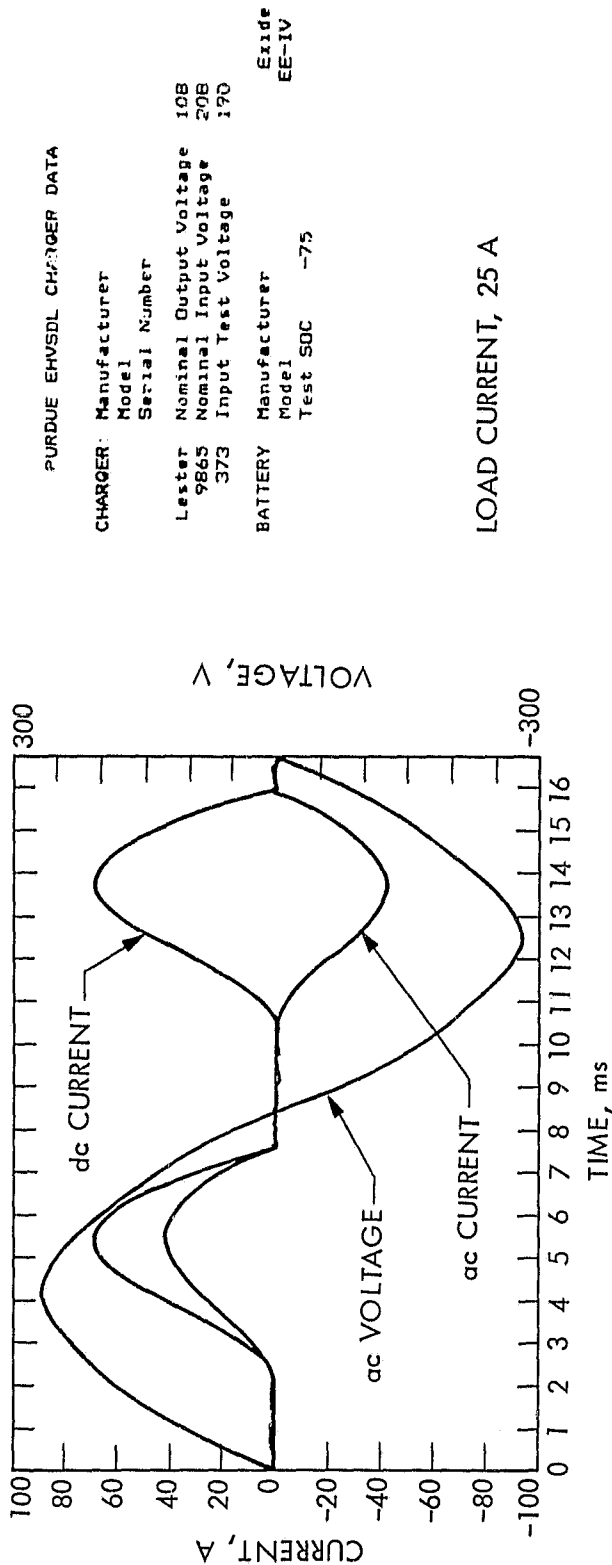
## CHARGER INPUT POWER WAVEFORM AND FOURIER ANALYSES VS. CHARGER LOAD CURRENTS



TEST RESULTS	
RMS LINE VOLTAGE	= 208.11
RMS LINE CURRENT	= 9.18
POWER IN, MAX	= 5814.71
POWER IN, MIN	= 236.46
POWER IN, AVE	= 1392.21
POWER IN @ 60 Hz	= 1406.91
POWER FACTOR @ 60 Hz	= 0.95
IVARS @ 60 Hz	= 467.32
POWER OUT, MAX	= 4987.78
POWER OUT, MIN	= -135.9C
POWER OUT, AVE	= 1178.88
EFFICIENCY	= 94.68
BATTERY CURRENT, MAX	= 33.90
BATTERY CURRENT, AVE	= 8.05
BATTERY CURRENT, RMS	= 16.60
MAX I/AVERAGE I	= 4.21
RIPPLE VOLTAGE	= 8.86
TOTAL HARMONIC DIST.	
FOR LINE CURRENT	= 80.80

AC VOLTAGE				FOURIER ANALYSIS				AC CURRENT			
Harmonic Number	Freq. Hz	Magnitude rms volts	% of Fund.	Phase degrees	Magnitude rms amps	% of Fund	Phase degrees	Phase difference			
1	60	207.90	100.00	0.58	7.14	100.00	-17.98	18.56			
2	120	2.31	1.11	76.25	0.08	1.09	19.80	-56.45			
3	180	1.70	0.82	-22.89	4.96	69.51	105.36	128.25			
4	240	0.19	0.09	-57.25	0.08	1.18	98.83	156.09			
5	300	5.05	2.43	1.03	2.75	38.48	-155.91	126.94			
6	360	0.27	0.13	40.33	0.07	1.00	145.17	179.50			
7	420	0.53	0.26	-136.87	0.77	10.72	-0.40	136.47			
8	480	0.12	0.06	-23.59	0.02	0.29	158.10	-168.31			
9	540	0.01	0.01	78.05	0.3	5.25	-37.17	115.22			
10	600	0.07	0.05	-43.18	0.02	0.30	-49.99	-4.80			
11	660	0.40	0.19	-11.59	0.52	7.25	90.97	102.56			
12	720	0.10	0.05	-29.95	0.03	1.60	25.54	55.49			
13	780	0.28	0.14	31.58	0.11	1.60	-166.46	161.96			
14	840	5.15	0.07	-55.76	0.00	0.06	24.36	80.12			
15	900	0.25	0.12	37.21	0.19	2.71	174.60	117.39			
16	960	0.13	0.06	-36.71	0.01	0.15	170.44	-152.85			
17	1020	0.07	0.04	106.07	0.18	2.52	-53.53	-159.59			
18	1080	0.19	0.09	-10.06	0.02	0.30	-38.58	-28.52			
19	1140	0.10	0.05	35.48	0.06	0.82	52.44	15.96			
20	1200	0.05	0.02	32.72	0.02	0.26	-103.15	-135.87			

Figure E-1. Waveform Data with Fourier Analysis Measurements (Load Current, 8 A)

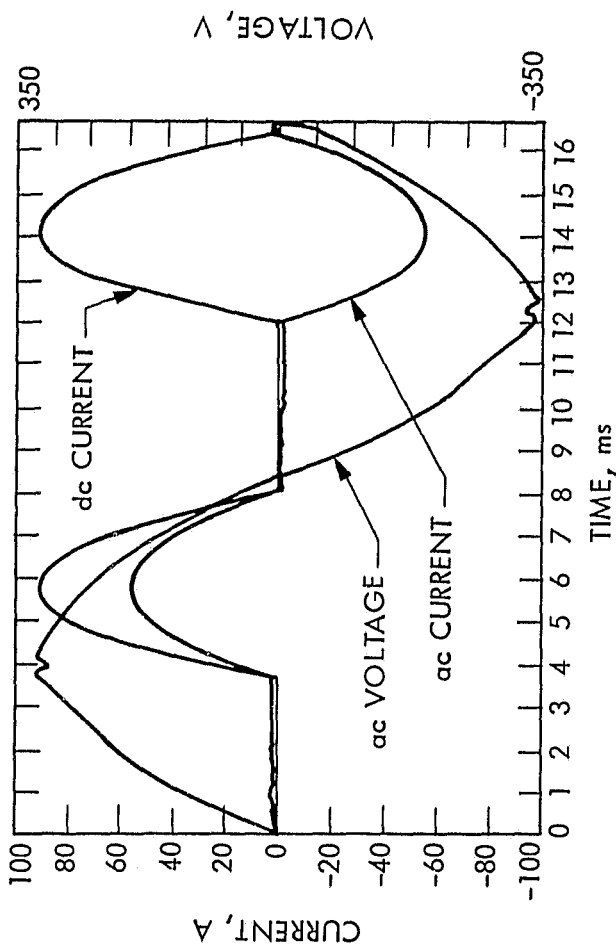


FOURIER ANALYSIS									
AC VOLTAGE					AC CURRENT				
Harmonic Number	Freq Hz	Magnitude rms volts	% of Fund	Phase degrees	Magnitude rms amps	% of Fund	Phase degrees	Phase difference	
1	60	190.63	100.00	0.60	20.43	100.00	-20.79	-1.38	
2	120	1.87	0.98	72.83	0.13	0.61	-12.80	85.83	
3	180	3.15	1.66	-19.94	9.43	46.27	106.81	126.75	
4	240	0.52	0.27	-1.87	0.05	0.23	79.62	81.49	
5	300	5.78	3.03	-12.25	1.19	5.82	176.68	-171.07	
6	360	3.33	0.17	27.45	0.03	0.16	72.97	45.52	
7	420	0.30	0.16	-139.52	1.01	4.96	-158.68	-19.16	
8	480	0.18	0.10	-4.01	0.03	0.11	104.00	108.02	
9	540	0.42	0.22	107.92	0.59	2.90	-133.12	118.96	
10	600	0.12	0.06	30.86	0.05	0.24	178.36	147.51	
11	660	0.22	0.11	83.51	0.35	1.70	-90.09	-173.60	
12	720	0.10	0.05	13.07	0.03	0.17	-131.02	-144.09	
13	780	0.17	0.09	151.39	0.28	1.39	-54.53	154.07	
14	840	0.11	0.06	44.86	0.03	0.15	-148.57	166.57	
15	900	0.26	0.13	163.45	0.20	0.98	-22.36	174.20	
16	960	0.13	0.07	7.09	0.03	0.12	-71.03	-78.12	
17	1020	0.20	0.11	-73.64	0.17	0.85	20.04	93.68	
18	1080	0.05	0.02	-53.66	0.03	0.12	-59.22	-1.56	
19	1140	0.10	0.05	-45.51	0.15	0.72	49.14	94.65	
20	1200	0.04	0.02	-49.84	0.03	0.13	-37.33	12.51	

TEST RESULTS									
IRMS LINE VOLTAGE	= 190.78								
IRMS LINE CURRENT	= 22.59								
POWER IN, MAX	= 10642.91								
POWER IN, MIN	= 158.32								
POWER IN, AVE	= 3492.37								
POWER IN @ 60 Hz	= 3627.02								
POWER FACTOR @ 60 Hz	= 0.93								
IVARS @ 60 Hz	= 1410.58								
POWER OUT, MAX	= 8672.16								
POWER OUT, MIN	= -35.72								
POWER OUT, AVE	= 3102.29								
EFFICIENCY	= 86.12								
BATTERY CURRENT, MAX	= 68.86								
BATTERY CURRENT, AVE	= 25.22								
BATTERY CURRENT, RMS	= 44.34								
MAX I/AVERAGE I	= 2.73								
RIPPLE VOLTAGE	= 11.67								
TOTAL HARMONIC DIST FOR LINE CURRENT	= 47.07								

Figure E-2. Waveform Data with Fourier Analysis Measurements  
(Load Current, 25 A)



# PURDUE EHVS DL CHARGER DATA

CHARGER: Manufacturer  
Model  
Serial Number  
Lester  
Nominal Output Voltage 108  
9865  
Nominal Input Voltage 208  
373  
Input Test Voltage 230

BATTERY: Manufacturer  
Model  
Test SOC --125  
Exide  
EE-IV

LOAD CURRENT, 32 A

TEST RESULTS	
RMS LINE VOLTAGE	= 229.93
RMS LINE CURRENT	= 29.54
POWER IN, MAX	= 15724.56
POWER IN, MIN	= 162.76
POWER IN, AVE	= 4867.44
POWER IN @ 60 Hz	= 4925.62
POWER FACTOR @ 60 Hz	= 0.83
IVARS @ 60 Hz	= 3315.30
POWER OUT, MAX	= 11769.31
POWER OUT, MIN	= -21.37
POWER OUT, AVE	= 4072.77
EFFICIENCY	= 83.57
BATTERY CURRENT, MAX	= 91.97
BATTERY CURRENT, AVE	= 31.90
BATTERY CURRENT, RMS	= 57.87
MAX 1/AVERAGE 1	= 2.88
RIPPLE VOLTAGE	= 15.35
TOTAL HARMONIC DIST	
FOR LINE CURRENT	= 14.65

FOURIER ANALYSIS									
AC VOLTAGE					AC CURRENT				
Harmonic Number	Freq Hz	Magnitude rms volts	% of Fund	Phase degrees	Magnitude rms amps	% of Fund	Phase degrees	Phase difference	
1	60	229.93	100.00	-0.46	25.95	100.00	-34.77	-34.26	
2	120	2.67	1.16	75.55	0.23	0.87	4.21	-71.34	
3	180	5.16	2.25	-54.67	13.81	53.22	69.73	124.40	
4	240	0.40	0.17	30.48	0.13	0.51	56.08	86.55	
5	300	7.68	3.34	-7.59	1.76	6.78	179.38	-173.03	
6	360	0.36	0.15	7.80	0.04	0.16	-4.51	-12.42	
7	420	1.27	0.56	-70.87	2.36	9.08	98.11	168.97	
8	480	3.27	1.42	-10.13	0.05	0.24	40.34	50.47	
9	540	0.43	0.19	66.89	0.47	1.81	-160.93	132.17	
10	600	0.20	0.09	19.49	0.03	0.11	44.90	54.39	
11	660	0.94	0.41	-0.38	0.99	3.81	134.45	134.83	
12	720	0.21	0.09	-13.51	0.06	0.23	41.87	75.47	
13	780	0.29	0.13	-3.71	0.12	0.47	-134.59	-130.98	
14	840	0.21	0.09	-20.54	0.03	0.11	50.59	71.13	
15	900	0.81	0.35	56.67	0.60	2.31	166.05	109.39	
16	960	0.18	0.08	-31.03	0.05	0.19	82.98	114.01	
17	1020	0.37	0.16	-5.30	0.03	0.10	130.95	136.25	
18	1080	0.23	0.10	-39.24	0.03	0.13	119.73	158.98	
19	1140	0.95	0.41	64.74	0.38	1.48	-164.47	130.79	
20	1200	0.13	0.06	-27.71	0.03	0.10	72.80	100.51	

Figure E-3. Waveform Data with Fourier Analysis Measurements  
(Load Current, 32 A)

ORIGINAL PAGE 13  
OF POOR QUALITY

## APPENDIX F

### OPERATION MANUAL, PARTS LIST, AND SCHEMATIC FOR MODEL 9865 LESTER CHARGER

Installation and Operating Instructions  
Lestronic Battery Charger  
Model 9865 - Type 108EL32-8ET  
Input: 115/208/230 Vac - 60 Hz  
Output: 108 Vdc, 32 A  
(With dc/dc converter power, 115-Vac fan output,  
and automatic start)

**Charger Location:** Make certain that the charger is located in the vehicle so that air flow to the charger fan is not restricted. Also, keep area around charger clean so that no debris can be pulled into the charger.

**Electrical Installation:** This charger is normally operated on one of the following 60-Hz, single-phase input voltages: 208 or 230 V.

**Caution:** It is imperative that the internal charger taps be set to the proper voltage range on which it will be operated. Severe damage to the charger and/or batteries may occur if the charger is operated on an improper voltage setting.

**Danger:** Due to the high voltages involved, the initial setup and servicing of the charger should be performed only by qualified personnel, and then only with ac power turned off and with the dc cord disconnected from the batteries.

**Input Voltage Settings:** The charger is shipped from the factory with the internal charger tap set for 220-240 V (230 V nominal) operation. If the charger is to be operated from a 200 to 220 V (208 V nominal) ac source, then change the tap as follows:

Remove the top cover from the charger. The internal charger taps are on a three-connection barrier strip located on top of the transformer assembly. Remove the screw retaining the tap lead and place the tap lead on the 208-V connection.

**For 115-Vac, 60-Hz, single-phase installation:** This charger may be operated from A 115-Vac source without any change required in the internal charger tap connections.

**Note:** The use of 115-Vac input should be limited to emergency situations and occasional charging when vehicle is not in use and a 208- or 230-V input is not available. Continual use of the 115-V input will lead to undercharging of the batteries, thus reducing performance and battery life.



Caution: Automatic shutoff of the charger will not occur in 115-V operation, and the charger will continue to operate until disconnected from the 115-V source at an output charging rate of approximately 6 A. The charger should not be allowed to operate under this condition for more than 24 h continuously to prevent possible damage to the batteries.

#### Operation:

- A. Plug the 115-V fan and vane-switch connector into the fan and vane-switch receptacle. The fan and vane-switch cable must be terminated at the correct terminals on the vane switch and fan (see schematic).
- B. Plug the dc/dc converter connector into the dc/dc converter receptacle. The dc/dc converter cable must be terminated at the correct terminals of the converter (see schematic).
- C. Plug the 108-V battery connector into the 108-V receptacle.
- D. Plug appropriate ac cord into proper charger receptacle.

Caution: To protect against shock hazards, connect ac cord only to properly grounded outlets.

Caution: When inserting the plug into the receptacle on the vehicle, be sure to twist the plug clockwise until it is firmly locked in place. If not, the elements of the connector may overheat, causing permanent damage to the plug and receptacle.

- E. Plug ac cord into 60-Hz, ac outlet. Charger will start immediately.

Note: Vane switch must close within 10 s after the charger starts and remain closed during the normal operation of the charger.

- F. Monitor ammeter for correct charge rate. When operating from a 208- or 230-V input, the initial charge rate will be approximately 32 A. The charge rate will gradually taper to a finish rate of approximately 8 A.

When operating from a 115-V input, the initial charge rate will be approximately 6 A and will remain in this range until the charger is shut off by disconnecting it from the ac source.

- G. Monitor Fans. Both the charger-mounted fan and the battery compartment fan must be operating while the charger is on, and the fan should continue to operate for a period of 1 h after the charger shuts off.
- H. Charger turns off automatically when batteries are fully charged (when operated from a 208- or 230-V ac source).

Caution: When operating from a 115-V ac source, shut off the charger manually by disconnecting it from the ac source.

Caution: Do not remove dc cord from batteries when charger is on. If charge cycle must be interrupted, disconnect ac cord before removing dc cord.

- I. Charge Time. When operating from a 208/230 Vac input, the charger requires 8 to 10 h under normal conditions to properly recharge the batteries. Cold batteries (below 50°F) or new batteries will require more time to achieve full charge.

Caution: When operating from a 115 Vac source, do not allow the charge time to exceed 24 h.

- J. Full Charge Test. (208/230-V input operation). To test for full charge on batteries, push "start" button. Charge rate should drop to 8 A and shut off within 45 to 90 min (new or cold batteries will require a longer period of time).

- K. Charger Overheats. If the internal temperature of the charger becomes too hot, the charger will automatically shut off and the red "over temperature" light on the front panel will glow. The fans will continue to operate for approximately 1 h after shutdown. To resume charging, the "temperature reset" button must be depressed and the charger restarted.

- L. After the completion of a normal battery charge, the charger may be restarted by pushing the "start" button (if the charger is still connected to the batteries and the ac source) or by removing and reinserting the ac cord into the 60-Hz, ac source.

Fuse Replacement: When replacing a fuse in the charger, always use the same type of fuse specified; otherwise, the charger or other wiring could be extensively damaged.

Table F-1. Replacement Parts List Lestronic Battery Charger<sup>a</sup>

Part Number	Description
9938	Case, Complete
9866	Transformer
7962	Heat Sink Assembly w/SCR
9983	SCR Assembly w/lead
2367	Ammeter, 0-50 A
8415	Capacitor, 20 Mfd.
4327	Shunt, Electronic
3853	Relay, 110 Vdc
3861	Relay, 12 Vdc
4633	Fuse Block for ac Fuses, 1 Pole
4632	End Barrier, for Fuse Block
4627	Fuse, FNW-30
4631	Fuse, FNW-20
4063	Fuse Base for Bussman Fuse
4692	Fuse, ANN-60
7965	Control Cable Assembly
7919	Receptacle Assembly, 6-Pin Receptacle
7998	Receptacle Assembly, 15-Pin Receptacle
8982	Lamp Assembly, Red
3837	Fuse Holder, Cartridge Type for 12 Vdc
4303	Fuse AGC-1
4687	Fuse AGC-2
4860	Fuse ABC-3
9872	Electronic Control Board, 108 Vdc
7810	Electronic Control Board, Fans, and Vane Switch
2807	Switch, Pushbutton
4726	Tap Strip
7957	Receptacle Assembly, dc
7958	Receptacle Assembly, ac
9973	Extension Cord, 115 Vac
9974	Extension Cord, 230 Vac
9975	Receptacle, Charger to Vehicle
9978	Cordset, dc (Battery to Charger)
4558	Relay, 120 Vac

<sup>a</sup> Model 9865 - Type 108EL32-8ET  
 Inut: 115/208/230 Vac - 60 Hz  
 Output: 108 Vdc, 32 A

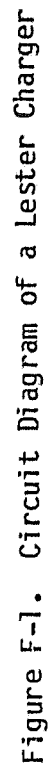


**Figure F-1. Circuit Diagram of a Lester Charger**